Miniaturized and modified QuEChERS method with mesostructured silica as clean-up sorbent for pyrrolizidine alkaloids determination in aromatic herbs

Sergio Izcara, Natalia Casado, Sonia Morante-Zarcero, Damián Pérez-Quintanilla, Isabel Sierra*

Departamento de Tecnología Química y Ambiental, E.S.C.E.T, Universidad Rey Juan Carlos, C/ Tulipán s/n, 28933 Móstoles, Madrid, Spain

* Corresponding author: Tel.: (+34) 914887018; fax: (+34) 914888143.

E-mail addresses: sergio.izcara@urjc.es; natalia.casado@urjc.es; sonia.morante@urjces; damian.perez@urjc.es; isabel.sierra@urjc.es

ABSTRACT

This work proposes the miniaturization and modification of the QuEChERS strategy using different large pore mesostructured silicas, non-modified and modified with amino groups (NH_2), as dispersive clean-up sorbents for multi-component extraction of 21 pyrrolizidine alkaloids from different aromatic herbs, combined with ultra-high performance liquid chromatography coupled to tandem mass spectrometry analysis. The procedure was miniaturized by reducing the amounts of sample (0.2 g), solvents (2 mL), clean-up sorbents (25 mg sorbent + 150 mg $MgSO_4$) and partitioning salts (0.65 g) employed. Best results were achieved using mesostructured silicas (LP-MS-NH_2) than conventional PSA. The method was validated (overall recoveries 73-105%) and applied to the analysis of 17 samples. All the samples were contaminated with PAs (average concentration 262 µg/Kg). Thyme and basil samples were the most contaminated, whereas rosemary was the least. Lasiocarpine, senecivernine N-oxide and europine N-oxide were the main PAs that contributed to their contamination.

Keywords: pyrrolizidine alkaloids; aromatic herbs; mesostructured silicas; µ-QuEChERS; UHPLC-MS/MS; food safety

1. Introduction

Pyrrolizidine alkaloids (PAs) and their oxidized forms (pyrrolizidine alkaloids *N*-oxides, PANOs) are natural plant toxins, which can be found as potential contaminants in food. Their intake is mainly associated with liver damage, among other health issues (Dusemund et al., 2018). The main sources of PAs consumption in humans are plant-derived products contaminated with these alkaloids due to the accidental inclusion of weeds or impurities from PAs-producing plants during harvest. Nonetheless, the horizontal natural transfer of PAs/PANOs through the soil among living plants growing nearby or from dead plant materials has also been demonstrated as an alternative contamination path (Selmar et al., 2015; Nowak et al., 2016; Selmar et al., 2019). In this sense, the European Food Safety Authority (EFSA) considers honey, teas, herbal teas and plant-derived food supplements as the main food products likely to be contaminated with PAs and PANOs (EFSA, 2017). However, recent food alerts have notified concerning high levels of these alkaloids in other matrices, such as spices and aromatic herbs, highlighting their occurrence as an important food safety issue that needs to be addressed urgently (RASFF, 2021). Nevertheless, to date, these matrices have gone mostly unnoticed, so works focusing on the detection of these contaminants in these food items are scarce in the literature (Cramer et al., 2013; Kapp, 2017; Picron et al., 2018a; Izcara et al., 2020; Kaltner et al., 2020). Thus, sensitive analytical methods need to be developed to accurately monitor the presence of these compounds in aromatic herbs and spices and ensure food safety. In this sense, due to their potential toxicity and their frequent occurrence, a regulation has recently been published to monitor the occurrence of PAs/PANOs in certain foodstuffs (COMMISSION REGULATION (EU) 2020/2040). In this regulation, maximum concentrations levels have been established for a total of 21 PAs/PANOs (intermedine, lycopsamine, senecionine, senecivernine, seneciphylline, retrorsine, echimidine, lasiocarpine, europine and heliotrine their corresponding N-oxides and senkirkine) (Figure 1) in some food products. As well, 14 additional PAs (known to co-elute with one or more of the above 21 compounds) can be also contemplated in these maximum concentration levels whenever the chromatographic method employed is able to individually

and separately identified them from the others (COMMISSION REGULATION (EU) 2020/2040). In fact, the coelution of isomers is the main challenge in the analysis of these contaminants. Moreover, the multiresidue determination of these natural contaminants in food samples is a difficult task, as they are subjected to multiple matrix interferences that hinder their extraction and detection because of the high complexity of food samples. Accordingly, a suitable clean-up procedure of the sample or sample extract before its instrumental analysis is crucial to achieve sensitive results and good analytical performance. In this context, the QuEChERS (quick, easy, cheap, effective, rugged and safe) procedure is an appropriate approach, as it involves simultaneous extraction and clean-up of samples and it is designed for the determination of multiple analytes at the same time (Anastassiades et al., 2003). In the original QuEChERS strategy, primary secondary amine (PSA) was used as dispersive clean-up sorbent, as it is useful to remove polar organic acids, polar pigments, some sugars and fatty acids due to its weak anion exchange properties. However, PSA is sometimes not capable of removing excessive interferences in complex matrices (Oellig & Schmid, 2019). For this reason, over the years, the QuEChERS method has been modified by the introduction of other clean-up sorbents, mainly, graphitized carbon black (GCB) and octadecylsilane (C18), which are usually used in combination with PSA (Bruzzoniti et al., 2014; Lawal et al., 2018). This has led researchers to search and evaluate other novel clean-up sorbents for QuEChERS. Consequently, multiwalled carbon nanotubes (MWCNTs) (Zhao et al., 2012; Han et al., 2015; Uclés et al., 2015), magnetic nanoparticles (Li et al., 2014; Zheng et al., 2015), zirconia-based sorbents (Uclés et al., 2015; Urban & Lesueur, 2017), sol-gel organic-inorganic hybrid sorbents (Omar, Irahim and Elbashir, 2014) and an organic polyamine polymer (Oellig & Schmid, 2019) have been proposed as alternative clean-up sorbents for QuEChERS. In this context, ordered mesostructured silicas are sol-gel materials with advanced textural properties (including high surface area, large pore volume, controllable particle size and morphology, well defined pore-size distribution, controllable wall composition, stable aqueous dispersion and excellent chemical, thermal and mechanical stability), making them suitable sorbents for sample preparation (Casado et al., 2017). Moreover, their surface can

be easily modified with a wide variety of ligands that can tailor their physical and chemical properties to specific applications. Thus, they can be designed to display different desirable characteristics in adsorption processes. Therefore, according to these advantageous properties, ordered mesostructured silicas could also be used as clean-up sorbents to isolate undesirable matrix interferences and enhance the sensitivity of analytical methods.

On the other hand, an important current trend in the analytical field is the development of environmentally friendly methodologies that comply with the Green Analytical Chemistry (GAC) principles, mainly involving a minimum consumption of solvents and samples. This can be achieved by the miniaturization of conventional analytical operations (Casado et al., 2020). In this context, the original QuEChERS procedure has been successfully miniaturized (µ-QuEChERS) and applied in different food matrices (Porto-Figueira, Camacho and Câmara, 2015; Casado et al., 2018; Izcara et al., 2020), leading to cost-effective and environmentally friendly methods. Accordingly, this work, proposes the miniaturization and modification of the original QuEChERS procedure by significantly reducing the amounts of sample, organic solvents, clean-up sorbents and partitioning salts required, and using different ordered mesostructured silicas as dispersive clean-up sorbents for the multi-component extraction of 21 PAs/PANOs from different aromatic herbs (rosemary, basil, thyme and herbs de Provence). To the best of our knowledge, this is the first time that ordered mesostructured silicas are used as dispersive clean-up sorbents in a miniaturized QuEChERS procedure for the determination of PAs and PANOs in food samples or other matrices.

2. Materials and methods

2.1. Chemicals, reagents and standard solutions

Poly(ethylene glycol)-block-poly(propyleneglycol)-block-poly(ethylene glycol) (EO20PO70EO20, Pluronic 123, M_{av}= 5800 g/mol, d = 1.019 g/mL), tetraethylorthosilicate (TEOS) 98% (M = 208.33 g/mol, d = 0.934 g/mL), decane (M = 142.28 g/mol, d = 0.73 g/mL) amd (3-aminopropyl)triethoxysilane

(M = 221.37 g/mol) were obtained from Sigma-Aldrich (St. Louis, MO, USA). HCl 37% (M = 36.46 g/mol, d = 1.19 g/mL), toluene, ethanol, ethyl ether, dimethyl sulfoxide (DMSO), acetonitrile (ACN) LC-MS grade, methanol (MeOH) LC-MS grade, sodium chloride (NaCl), anhydrous magnesium sulphate ($MgSO_4$), sodium citrate dibasic sesquihydrate, sodium citrate tribasic dehydrate and PSA sorbent were acquired from Scharlab (Barcelona, Spain). Ammonium acetate LC-MS grade and formic acid LC-MS grade were purchased from Fluka (Busch, Switzerland). Ammonium fluoride was from Panreac Química (Castellar del Vallès, Barcelona, Spain). A Millipore Milli-Q-System (Billerica, MA, USA) was used for water (resistivity 18.2 MW cm).

Standards of PAs and PANOs with high purity grade (≥90%) were supplied by PhytoLab GmbH & Co. KG (Vestenbergsgreuth, Germany). Only retrorsine was acquired from Sigma-Aldrich (St. Louis, MO, USA). Individual standard solutions (1000 µg/mL) were prepared according to the solubility of each compound. Thus, intermedine, lycopsamine, retrorsine, seneciphylline, senecionine, heliotrine, heliotrine *N*-oxide, europine and europine *N*-oxide were prepared in ACN/DMSO (4/1, v/v), whereas senkirkin, senecivernine, senecivernine *N*-oxide, echimidine, echimidine *N*-oxide, lasiocarpine, lasiocarpine *N*-oxide, intermedine *N*-oxide, lycopsamine *N*-oxide, retrorsine *N*-oxide, seneciphylline *N*-oxide and senecionine *N*-oxide were prepared in MeOH. From the individual solutions, a standard solution containing all the 21 analytes at 1 µg/mL (each of them) was prepared in water. This multicomponent solution was used to achieve working standard solutions at different concentration levels by appropriate dilution with water to carry out the analytical performance of the method. All the standard solutions were stored at -20 ºC.

2.2.Synthesis and characterization of LP-MS and LP-MS-NH_2 mesostructured silicas

The large-pore mesostructured silica was synthetized as follows: Pluronic 123 (12 g) was dissolved in 0.1% HCl (420 mL). The solution was stirred until homogenization at 30 ºC. Then, ammonium fluoride (0.14 g) was added and stirred for 10 min. Subsequently, TEOS and decane (25.84 g and 75

130 mL, respectively) were added, drop by drop, to the mixture, which was stirred for 20 h at 30 ºC. After
131 this reaction time, the mixture was transferred with 25 mL of Milli-Q water to an autoclave reactor and
132 heated at 100 ºC for 48 h. The solid product was recovered by filtration and washed with Milli-Q water.
133 Finally, it was calcinated at 540 ºC for 8 h to remove the residual surfactant. The resultant material was
134 denoted as LP-MS. Subsequently, 3 g of LP-MS were weighted and mixed with toluene (40 mL). 3 mL
135 of (3-aminopropyl)triethoxysilane were added and the mixture was stirred at 80 ºC for 24 h in a silicone
136 bath and under nitrogen atmosphere. The material was recovered by filtration and was washed
137 successively with toluene, ethanol and of ethyl ether (40 mL of each one). Finally, the material was dried
138 at 50-60 ºC overnight and denoted as LP-MS-NH_2.

139 Both materials were characterized. The data and results related to the characterization assays are
140 included in the Supplementary Material (see SM1).

141 *2.3.Samples*

142 Dried aromatic herbs samples, including rosemary, basil, thyme, and herbs de Provence, with
143 different types of farming (conventional or organic) and from different geographical origins were
144 acquired at local supermarkets in Madrid (Spain). Sampling was performed according to the European
145 Commission Regulation No. 401/2006 concerning sampling and analysis of mycotoxins in foodstuff. In
146 this sense, 5 sub-samples were acquired for each lot number. Additionally, a rosemary sample and a
147 basil sample were collected from plants grown "in-house" in individual pots, from Toledo (Spain) and
148 Madrid (Spain), respectively. These samples were collected from the plants and dried for their analysis.
149 Also, a thyme sample on the branch was collected from a wild crop field in Cádiz (Spain). Sample details
150 are shown in Table S1 of the Supplementary Material. Samples were denoted by indicating in the first
151 letter the type of aromatic herb (*R* for rosemary, *B* for basil, *T* for thyme, and *H* for herbs de Provence)
152 followed by a dash with their type of farming (*C* for conventional, *O* for organic and *W* for wild farming,
153 whereas *I* was for samples collected from plants grown "in-house"). All samples were separately milled

to a fine powder with a grinder (A11 basic analytical mill, IKA® - Werke GmbH & Co. KG, Staufen, Germany) for their homogenization and stored until their analysis. Each sample was analyzed in triplicate.

2.4. Modified µ-QuEChERS procedure

The miniaturization of the QuEChERS procedure was based on a previous work of our research group carried out for oregano samples (Izcara et al., 2020), with modifications: 1 mL of water was added to 0.2 g of dry sample (previously weighted) for hydration of the sample matrix. This mixture was vortexed for 1 min and then was magnetically stirred for 30 min. Subsequently, 1 mL of ACN was added to the mixture, vortexed for 1 min and magnetically stirred for 30 min. Then, 0.65 g of the partitioning salts mixture ($MgSO_4$, NaCl, sodium citrate tribasic dehydrate and sodium citrate dibasic sesquihydrate in proportion 4:1:1:0.5) were added and vortexed for 1 min, followed by ultrasound agitation (5 min) and centrifugation (10 min at 6000 rpm). The upper part of the supernatant corresponding to the ACN fraction was separated and collected, while the rest of the sample extract was re-extracted again with 0.5 mL of ACN, vortexed for 1 min, ultrasound assisted (5 min) and centrifuged (10 min at 6000 rpm). The aliquot from the upper part of the supernatant corresponding to the ACN fraction was collected with the previous one and transferred to an Eppendorf containing 150 mg of $MgSO_4$ and 25 mg of the clean-up sorbent (LP-MS, LP-MS-NH_2 or PSA). This mixture was vortexed for 1 min and centrifuged (5 min at 10,000 rpm). The supernatant was collected in a chromatographic vial, and the residue was re-extracted again with 250 µL of ACN, vortexed for 1 min and centrifuged (5 min at 10,000 rpm). The supernatant was collected with the previous one in the vial and filtered through a 0.45 µm PTFE filter membrane for its subsequent injection in the chromatographic system.

2.5.UHPLC-MS/MS analysis

An UHPLC system (Dionex UltiMate 3000, Thermo Scientific, Waltham, MA, USA) coupled to an ion-trap tandem mass spectrometer detector (ESI-ITMS amaZon SL, Bruker) was used for analysis.

Parameters for mass spectrometry acquisition were set as follows: electrospray ionization interface (ESI) in positive ion mode, capillary voltage −4500 V, end plate offset −500 V, nebulizer gas 20 psi, dry gas 10 L/min and dry temperature at 200 °C. Multiple reaction monitoring (MRM) scan mode was used for all analytes. The ESI source parameters for each analyte were determined by direct infusion of individual standard solutions (5 µg/mL) at a flow rate of 4 µL/min. By individually infusing the analytes, is was possible to identify the precursor ion of each analyte ($[M+H]^+$) in positive ion mode. Then, this precursor ion was isolated and fragmentated to obtain the corresponding product ions of each analyte. In this sense, MS^2 was performed, and through the software of the mass spectrometer the extracted ion scan chromatograms were obtained with the mass spectrum of each analyte. The chromatographic separation of the 21 PAs/PANOs was carried out according to our previous work (Izcara et al., 2020), using a Luna Omega Polar C18 column (100 mm x 2.1 mm, 1.6 µm particle size, Phenomenex, Torrance, CA, USA) at 25 ºC and a gradient elution. The mobile phase included water containing 0.2% formic acid and 5 mM ammonium acetate (solvent A) and MeOH containing 10 mM ammonium acetate (solvent B). The gradient conditions were: 5% B (0–0.5 min), 5–50% B (0.5–7 min), 50% B (7–7.5 min), 50–100% B (7.5–11 min), 100% B (11–12 min), 100–5% B (12–14 min) and re-equilibration of 1 min to initial conditions, yielding a total analysis time of 15 min. The flow rate was 0.250 mL/min, and the injection volume 2 µL. Retention time and mas spectrum parameters are presented in Table 1. For the identification and confirmation of the compounds, the most intense product ion obtained for each analyte in its mass spectrum (MS^2) was used for quantification, while the other product ions obtained were monitored for confirmatory purposes.

2.6.Assessment of analytical parameters

Several analytical parameters were determined for method evaluation and method validation. These parameters were assessed following the criteria described in the SANTE/12682/2019 document, in regulation EC No 401/2006, and in the Q2(R1) ICH guidelines (International Council for Harmonisation 2005), since there is currently no official regulation for the validation of analytical methods to monitor

the presence of PAS/PANOs in food or feed. Accordingly, linearity was assessed with matrix-matched calibration curves prepared in three consecutive days. These curves were prepared for each matrix at six known concentration levels within the linear range evaluated. For this purpose, the sample extracts obtained after the µ-QuEChERS procedure were spiked with an aliquot of a standard solution containing the target analytes according to the desired concentration level of the calibration curve. Likewise, an unspiked sample extract (denoted blank sample) also subjected to the µ-QuEChERS procedure was analyzed in case some analytes were found in the sample in a natural way, so their signal could be subtracted. The criteria for good linearity involve coefficient of determination (R^2) values closed to 1 and values $\leq \pm$ 20% for the deviation of the back-calculated concentrations of the calibration standards from the true concentrations (SANTE/12682/2019; EC No 401/2006). Matrix effects were determined by comparing the slopes of the calibration equations obtained from both matrix-matched and solvent-based calibration curves (both expressed in the same units µg/L), calculating the ratio slope matrix-matched/slope solvent-based*100 for each of the 21 analytes. A ratio lower than 100% suggests signal suppression, whereas a ratio greater than 100% indicates signal increase. When the value is in the range of 80-120%, the matrix effects can be ignored. However, when the signal suppression or enhancement is greater than this margin of 20%, matrix effects must be considered in calibration (European Commission SANTE/12682/2019). Nonetheless, values within a margin ± 40% could be determined as soft matrix effects, but they need to be considered in calibration.

The selectivity of the method was determined by comparing the spectra of the different analytes obtained from standard solutions with the spectra obtained in the samples. It was considered satisfactory when the variation in the spectra was less than ± 30 % and the retention time of the analytes was within the interval ± 2.5 % (European Commission SANTE/12682/2019). The sensitivity of the method for each matrix was determined through the method detection limits (MDLs) and method quantification limits (MQLs) of the analytes. These limits were estimated based on the standard deviation of the

response and the slope obtained in the matrix-matched calibration curves for the lowest concentration level (Q2(R1) International Council for Harmonisation, 2005):

MDL= 3.3 x standard deviation of the response at the lowest concentration / slope of the calibration curve

MQL= 10 x standard deviation of the response at the lowest concentration / slope of the calibration curve

The recovery assays were assessed by comparing the areas obtained for samples spiked with a known concentration of analytes and subjected to the µ-QuEChERS procedure with those areas obtained for simulated samples (samples spiked at the same concentration but at the end of the µ-QuEChERS procedure prior to their chromatographic analysis). For method evaluation, the recovery assays were performed spiking the aromatic herb samples at a concentration of 100 µg/Kg. A maximum concentration of 400 µg/Kg of total PAs and PANOs has been established for dried herbs (excluding borage, lovage, marjoram and oregano, for which a maximum concentration of 1000 µg/Kg is set) (COMMISSION REGULATION (EU) 2020/2040). Therefore, for method validation, the accuracy was evaluated in terms of recovery for the aromatic herb matrices at three concentration levels: low (10 µg/Kg), medium (100 µg/Kg) and high (800 µg/Kg), so that this value can be covered in a wide range. These results were expressed as the mean recovery obtained from six samples (n = 6) spiked with the analytes at the corresponding concentration (low, medium or high) and subjecting them to the proposed extraction procedure. According to the validation guidelines, the recovery values should be between 70 and 120% (SANTE/12682/2019; EC No 401/2006). On the other hand, the method precision was evaluated in terms of repeatability and reproducibility, using the same validation levels (low, medium and high) than for the accuracy. For repeatability (expressed as RSD%), a sample spiked with the analytes at the corresponding validation level was consecutively injected six times (n = 6) on the same day. The reproducibility (also expressed as RSD%) was calculated by the analysis of three replicates of a sample (spiked with the analytes at the corresponding validation level), which were injected in

triplicate throughout three different days (n = 9). According to the validation guidelines, the RSD values for these precision parameters should be ≤ 20% (SANTE/12682/2019; EC No 401/2006).

The validation of the method was carried out for each matrix using a representative sample of each of the aromatic herbs. As no blank samples or certified materials were available, the validation was carried out with samples R-C-1, B-C-1 and T-C-1 for rosemary, basil and thyme matrices, respectively. As the herbs de Provence are a mixture of different aromatic herbs (Table S1), this type of matrix was not validated. Nevertheless, some analytical parameters of this matrix were assessed with sample H-O-2, such as linearity, MDLs, MQLs, and the accuracy at one level (Table S2).

2.7.Statistical Analysis

Each aromatic herb sample was analyzed in triplicate. The statistical analysis of the samples was performed with SPSS 19.0 software, using one-way analysis of variance (ANOVA) and Duncan multiple range test (significant differences at $p \leq 0.05$).

3. Results and discussion

3.1. Evaluation of clean-up sorbents and optimization of the µ-QuEChERS procedure

The mesostructured silicas synthesized (LP-MS and LP-MS-NH_2) and a commercial PSA were evaluated as clean-up sorbents under same conditions. For this purpose, these materials were initially tested in the clean-up step of the µ-QuEChERS procedure described in our previous work (Izcara et al., 2020). The miniaturization of this method provides a cost-effective and environmentally friendly microextraction that enables to improve the original QuEChERS strategy, as it successfully reduces the amounts of sample, solvents, clean-up sorbents and partitioning salts employed, as previously described in Section 2.4. Accordingly, after analytes were extracted with 1 mL of ACN followed by partitioning of the analytes in the presence of a salt mixture ($MgSO_4$, NaCl, sodium citrate tribasic dehydrate and sodium citrate dibasic sesquihydrate in proportion 4:1:1:0.5), the ACN phase was further cleaned up

with anhydrous $MgSO_4$ and 25 mg of clean-up sorbent (PSA, LP-MS or LP-MS-NH_2). The clean-up efficiency of the materials was assayed through the determination of matrix effects and the method recoveries as explained in Section 2.6. These preliminary studies were carried out with rosemary and basil (R-C-1 and B-C-1, respectively). As shown in Figure 2a and Table S3 most of the compounds presented significant matrix effects in both matrices with the three materials tested, as they showed values lower than 80%. In general, matrix effects were stronger with PSA than with LP-MS and LP-MS-NH_2 in both samples (Figure 2a, Table S3), suggesting that the clean-up efficiency of mesostructured silicas was higher than the one achieved with PSA. Therefore, it was confirmed that mesostructured silicas can be useful clean-up sorbents. Regarding both silicas, LP-MS-NH_2 provided less matrix effects than LP-MS, as more analytes had values in the range 80-120% (Figure 2a, Table S3). Therefore, LP-MS-NH_2 seemed to be the most suitable clean-up sorbent, as fewer analytes were affected by the matrix interferences when using this material (Figure 2a, Table S3). Nevertheless, regarding the recovery values, although they followed a similar trend among the three materials in the rosemary matrix, for some analytes the recoveries were low (<60%), such as for: intermedine, retrorsine, europine, lycopsamine, senkirkin, intermedine *N*-oxide, seneciphylline, echimidine *N*-oxide, europine *N*-oxide and lycopsamine *N*-oxide (Figure S1). The recoveries in basil were also similar among the three sorbents, but some of them were also below the 60% (intermedine, europine, lycopsamine and their corresponding *N*-oxides) (Figure S2). These low recovery values observed for some of the analytes were generally obtained with all three sorbents in both matrices (Figures S1 and S2). It was observed that the most polar analytes (those that eluted in the chromatogram first) were the ones with the lowest recovery values, but at the same time were the ones with the less matrix effects. This may suggest that the sorbent materials employed have more affinity to retain interferences of polar type because of the polar properties of the chemical structure of the silicas. In fact, PSA is indicated for removing polar organic acids, polar pigments and sugars. Therefore, the most polar PAs can also be retained in the material, and for this reason, probably lower recovery values were achieved for them. Overall, despite the low

recovery values achieved for some analytes, as LP-MS-NH_2 seemed to provide less matrix effects in both samples (Figure 2a, Table S3), it was selected as the most suitable clean-up sorbent (Figure 2a, Table S3). Nonetheless, with the aim of improving the recovery values, some modifications in the µ-QuEChERS procedure were performed for its optimization. These modifications included a second extraction cycle with 0.5 mL of ACN before the clean-up procedure and an elution step with 250 µL of ACN after the clean-up step, as explained in section 2.4. As shown in Figure 2b and c, with these modifications the recoveries in the rosemary and basil samples were significantly improved in almost all the analytes. The overall recoveries for rosemary with the new extraction conditions ranged from 67 to 107% (Figure 2b), whereas in the basil matrix they ranged from 78 to 105% (Figure 2c).

Finally, under these final extraction conditions, the method recoveries were also assayed for a thyme sample (T-C-1) and an herb de Provence sample (H-O-2) (Figure S3). As it can be observed, good recoveries were achieved for all the analytes in the thyme sample, ranging from 75 to 106% (Figure S3a). In contrast, the recoveries in the herbs de Provence matrix range from 79 to 103% (Figure S3b), Therefore, in general, good recovery values were achieved for all the PAs/PANOs analyzed in the different herb matrices. Thus, it was confirmed that LP-MS-NH_2 could be effectively used as clean-up sorbent in the different aromatic herb samples.

3.2.Method validation

Once LP-MS-NH_2 was selected as the most efficient clean-up sorbent, the method was validated in terms of linearity, selectivity, MDLs, MQLs, accuracy and precision. Good analytical performance of the method was achieved for the three aromatic herbs. As it can be observed in Tables 2-4, all compounds showed good linear regression, with coefficient of determination (R^2) values > 0.998. Moreover, values (%) of the deviation of the back-calculated concentrations ranged from -11 to +19% for rosemary and basil, and from -20 to +19% for thyme. Therefore, this parameter was successfully achieved in the three matrices, as the values were in all cases ≤ ± 20% (SANTE/12682/2019). In addition, the deviation (as

RSD%) of the slopes of the matrix-matched calibration curves prepared in three consecutive days ranged from 0.5 to 8%. Good selectivity of the method was achieved, as the deviation of the ion ratios obtained in the different samples did not deviate more than ± 30% in comparison to the mass spectra obtained with standard solutions. Moreover, the retention time of all the analytes was within the interval ± 2.5%. MDLs of the analytes were in the range 0.7-3.0, 0.7-3.0 and 0.4-2.9 µg/Kg, and MQLs 2.5-9.9, 2.2-10.0 and 1.2-9.7 µg/Kg for rosemary, basil and thyme, respectively (Table 2-4). On the other hand, the overall average recoveries obtained for the three validation levels were in the range 79-103%, 88-103% and 73-105% for rosemary, basil and thyme respectively (Tables 2-4). Therefore, this validation parameter was successfully accomplished as all the values were within the range 70-120% (SANTE/12682/2019; EC No 401/2006). Likewise, satisfactory precision values were obtained at the three validation levels in the three matrices, as all of them were ≤ 20% (Tables 2-4). Therefore, as the validation guidelines were fully accomplished, the analytical performance of the µ-QuEChERS procedure proposed was successfully demonstrated. Thus, this procedure can be reliably applied to the analysis of PAs and PANOs in aromatic herb samples.

3.3.Analysis of samples

The feasibility of the method was demonstrated by its application to the analysis of 17 samples, including 4 rosemary samples, 5 basil samples, 4 thyme samples and 4 herbs de Provence samples (Figure 3). The quantification was performed with the matrix-matched calibration curves calculated for each type of aromatic herb matrix. Contents below the MDL were considered as 0.0 µg/Kg (not detected), whereas contents between the MDL and the MQL were included as <MQL (Table S4). As it can be observed in Figure 3, all the samples analyzed were contaminated with PAs and PANOs, but all the 21 target analytes were not always found in all the samples. According to COMMISSION REGULATION (EU) 2020/2040, the maximum amount of PAs/PANOs allowed in dried herbs (except for borage, lovage, marjoram and oregano) is 400 µg/Kg. Accordingly, all the samples analyzed were below this limit, except two thyme samples: T-C-1 (447 µg/Kg) and T-O-1 (553 µg/Kg) (Figure 3a).

Conversely, the smallest average content (49 µg/Kg) was found in a rosemary sample (R-C-2) (Figure 3a). Based on the structural and botanical origin, PAs/PANOs can be classified in four different families (heliotrine-type, senecionine-type, lycopsamine-type and monocrotaline-type) (Picron et al., 2018a). Accordingly, heliotrine-type PAs (particularly, lasiocarpine, lasiocarpine *N*-oxide and europine *N*-oxide) were the ones which significantly contributed to the contamination of the aromatic herb samples analyzed, as they were often found in the samples at a relatively higher concentration value than the other PAs/PANOs, followed by the senecionine-type PAs (mainly, senecivernine *N*-oxide and senecionine *N*-oxide) (Figure 3b). This contamination profile matches with the one described by other authors in previous works (Picron et al., 2018a; Kaltner et al., 2020). The occurrence of heliotrine-type compounds is usually related to co-harvesting or adulteration with *Heliotropium spp.* and *Borago spp.*, whereas the contamination with senecionine-type PAs is often associated to species of the Asteraceae family, mainly *Senecio vulgaris (*Picron et al., 2018a; Kapp, Hägele, and Plate, 2019; Kaltner et al., 2020). Regarding lycopsamine-type PAs, only the occurrence of echimidine was relevant in some of the samples analyzed (R-C-3, T-C-1, T-W-1, H-C-1 and H-C-2) (Figure 3b), which may indicate contamination with plants belonging to the Boraginaceae family, such as *Borago spp* (Kaltner et al., 2020; Mädge et al., 2020). Thyme and basil samples were the most contaminated samples, with an average content of PAs/PANOs of 394.25 and 293.40 µg/Kg, respectively. In contrast, rosemary samples were the least contaminated, with an average content of PAs/PANOs of 148.25 µg/Kg (Figure 3a). The herbs de Provence are a mixture of different aromatic herbs (Table S1), so their contamination can be due to more than one aromatic herb. In this sense, this mixture of herbs also contains oregano, which is one of the culinary herbs for which most of the food alerts related to concerning high values of PAs/PANOs have been notified (Izcara et al., 2020). Accordingly, several works in the literature have reported high levels of PAs and PANOs in oregano samples (Kapp, Hägele, and Plate, 2019; Kaltner et al., 2020; Izcara et al., 2020). However, despite their content in oregano and other herbs (Table S1), the

herbs de Provence samples analyzed in this work showed an average value of PAs/PANOs of 203.50 µg/Kg, which is lower than the ones obtained for other herbs such as thyme and basil (Figure 3a).

The samples grown "in-house" in a private garden were expected not be contaminated. However, these samples were also positive, although, in general, they were less contaminated that the samples acquired from the supermarket (Figure 3a). The contamination pattern among these sample was very similar, with senecivernine *N*-oxide, lasiocarpine and europine *N*-oxide as the main compounds that contributed to their contamination (Figure 3b). The occurrence of these alkaloids in the "in-house" samples reinforces the horizontal natural transfer of PAs/PANOs through the soil among living plants growing nearby or from dead plant materials (Selmar et al., 2015; Nowak et al., 2016; Selmar et al., 2019), since the soil and compost employed in the pots of these plants had previously been used to grow other types of plants, which could be PAs-producing plants or be contaminated with weeds containing PAs /PANOs. Moreover, the thyme sample collected from a wild field showed significantly higher PAs/PANOs contamination values that the samples "in-house" (Figure 3a), probably because it was more exposed to fields of PAs-producing plants growing nearby, what reassert the horizontal natural transfer as contamination path of PAs/PANOs. In fact, in this wild sample the occurrence of some lycopsamine-type alkaloids, such as lycopsamine *N*-oxide and intermedine *N*-oxide, stood out compared to the other samples analyzed, in which in most of them these compounds were not even present (Figure 3b). This highlights the wide variety of unexpected botanical species that may contaminate these herbs.

Regarding the type of farming, it was not possible to draw significant conclusions. Among the basil samples, no significant differences were observed between the samples produced by conventional and organic farming, as the total amount of PAs/PANOs was very similar among them (Figure 3a). It was only noticed that seneciphylline *N*-oxide was only found in the conventional farming samples, whereas europine was only in the organic farming samples (Figure 3b). In the case of the herbs de Provence samples, the ones obtained by organic farming were less contaminated than the ones with conventional farming (Figure 3a). However, in the thyme samples, the sample most contaminated was one produced

by organic farming (T-O-2), which in fact was the sample that presented the highest contamination value (553 µg/Kg) of all the aromatic herbs analyzed (Figure 3a). Moreover, in general, all the aromatic herbs presented the same contamination profile regardless of their type of farming (Figure 3b).

4. Conclusions

The original QuEChERS strategy was successfully miniaturized by reducing the amounts of sample (0.2 g), solvents (2 mL), clean-up sorbents (25 mg sorbent + 150 mg MgSO4) and partitioning salts (0.65 g) employed, leading to an improved cost-effective and environmentally friendly microextraction method, which meets the Green Analytical Chemistry principles. Moreover, it was confirmed that mesostructured silicas could be considered as promising and alternative clean-up sorbents in sample preparation. The feasibility of the method proposed with LP-MS-NH_2 was determined by its validation and its application to the analysis of 17 different aromatic herbs. All the samples analyzed were contaminated with PAs and PANOs, but only in two thyme samples the sum of the total PAs/PANOs exceeded 400 µg/Kg, which is the maximum limit regulated for these compounds in aromatic herbs. In general, all the aromatic herbs presented the same contamination profile regardless of their type of farming. Heliotrine-type PAs were the ones which significantly contributed to the contamination of the aromatic herb samples analyzed, followed by the senecionine-type PAs, whereas the occurrence of lycopsamine-type PAs was less significant. In this sense, lasiocarpine, europine *N*-oxide and senecivernine *N*-oxide were the PAs that significantly contributed to the contamination of the samples analyzed. In addition, the horizontal natural transfer of PAs/PANOs through the soil among living plants growing nearby or from dead plant materials was reinforced as possible contamination path through the analysis of samples cultivated “in-house” and collected from wild fields. Overall, this work confirmed the concerning occurrence of these contaminants in aromatic herbs, highlighting the need to develop analytical strategies that enable to monitor and regulate the presence of these contaminants in food items to ensure the safety of consumers.

Author Contributions: Conceptualization, I.S. and S.M.-Z.; methodology, S.I., N.C. and D.P-Q; validation, S.I.; formal analysis, S.I.; investigation, N.C.; resources, S.I., N.C. and D.P.; data curation, S.I., N.C., S.M.-Z. and D.P-Q.; writing—original draft preparation, N.C.; writing—review and editing, N.C., S.M.-Z., D.P-Q and I.S.; visualization, S.I. and N.C.; supervision, S.M.-Z. and I.S.; project administration, S.M.-Z.; funding acquisition, I.S. All authors have read and agreed to the published version of the manuscript.

Funding: This research was funded by MCIU/AEI/FEDER, UE, project number RTI2018-094558-B-I00.

Conflicts of interest: The authors declare no conflict of interest. The funders had no role in the design of the study; in the collection, analyses, or interpretation of data; in the writing of the manuscript, or in the decision to publish the results.

References

Anastassiades, M., Lehotay, S. J., Štajnbaher, D., & Schenck, F. J. (2003). Fast and easy multiresidue method employing acetonitrile extraction/partitioning and "dispersive solid-phase extraction" for the determination of pesticide residues in produce. *J. AOAC Int.*, *86*, 412–431. https://doi.org/10.1093/jaoac/86.2.412

Bruzzoniti, M. C., Checchini, L., De Carlo, R. M., Orlandini, S., Rivoira, L., & Del Bubba, M. (2014). QuEChERS sample preparation for the determination of pesticides and other organic residues in environmental matrices: a critical review. *Anal. Bioanal. Chem.*, *406*, 4089-4116. https://doi.org/10.1007/s00216-014-7798-4

Casado, N., Gañán, J., Morante-Zarcero, S., & Sierra, I. (2020). New advanced materials and sorbent-based microextraction techniques as strategies in sample preparation to improve the determination of natural toxins in food samples. *Molecules*, *25*, 702. https://doi.org/10.3390/molecules25030702

Casado, N., Perestrelo, R., Silva, C. L., Sierra, I., & Câmara, J. S. (2018). An improved and miniaturized analytical strategy based on μ-QuEChERS for isolation of polyphenols. A powerful approach for quality control of baby foods. *Microchem. J.*, *139*, 110-118. https://doi.org/10.1016/j.microc.2018.02.026

Casado, N., Pérez-Quintanilla, D., Morante-Zarcero, S., & Sierra, I. (2017). Current development and applications of ordered mesoporous silicas and other sol–gel silica-based materials in food sample preparation for xenobiotics analysis. *TrAC*, *88*, 167-184. https://doi.org/10.1016/j.trac.2017.01.001

COMMISSION REGULATION (EU) 2020/2040 of 11 December 2020 amending Regulation (EC) No 1881/2006 as regards maximum levels of pyrrolizidine alkaloids in certain foodstuffs. Retrieved from https://eur-lex.europa.eu/legal-content/EN/TXT/PDF/?uri=CELEX:32020R2040&from=ES Accessed December 2, 2021.

Cramer, L., Schiebel, H. M., Ernst, L., & Beuerle, T. (2013). Pyrrolizidine alkaloids in the food chain: Development, validation, and application of a new HPLC-ESI-MS/MS sum parameter method. *J. Agric. Food Chem., 61*, 11382–11391. https://doi.org/10.1021/jf403647u

Dusemund, B., Nowak, N., Sommerfeld, C., Lindtner, O., Schäfer, B., & Lampen, A. (2018). Risk assessment of pyrrolizidine alkaloids in food of plant and animal origin. *Food Chem.Toxicol., 115*, 63–72. https://doi.org/10.1016/j.fct.2018.03.005

European Commission Regulation No. 401/2006 of 23 February 2006 laying down the methods of sampling and analysis for the official control of the levels of mycotoxins in foodstuffs. Retrieved from https://eur-lex.europa.eu/legal-content/EN/TXT/PDF/?uri=CELEX:32006R0401&from=EN Accessed July 29, 2021.

European Commission SANTE/12682/2019. *Guidance Document on Analytical Quality Control and Method Validation Procedures for Pesticide Residues and Analysis in Food and Feed*. Retrieved from https://www.eurl-pesticides.eu/userfiles/file/EurlALL/AqcGuidance_SANTE_2019_12682.pdf Accessed December 16, 2021.

European Food Safety Authority. (2017). Risks for human health related to the presence of pyrrolizidine alkaloids in honey, tea, herbal infusions and food supplements. *EFSA J., 15*, 4908. https://doi.org/10.2903/j.efsa.2017.4908

Han, Y., Zou, N., Song, L., Li, Y., Qin, Y., Liu, S., Li, X., & Pan, C. (2015). Simultaneous determination of 70 pesticide residues in leek, leaf lettuce and garland chrysanthemum using modified QuEChERS method with multi-walled carbon nanotubes as reversed-dispersive solid-phase extraction materials. *J. Chromatogr. B, 1005*, 56-64. https://doi.org/10.1016/j.jchromb.2015.10.002

Izcara, S., Casado, N., Morante-Zarcero, S., & Sierra, I. (2020). A Miniaturized QuEChERS Method Combined with Ultrahigh Liquid Chromatography Coupled to Tandem Mass Spectrometry for the

478 Analysis of Pyrrolizidine Alkaloids in Oregano Samples. *Foods, 9*, 1319.
479 https://doi.org/10.3390/foods9091319

480 Kaltner, F., Rychlik, M., Gareis, M., & Gottschalk, C. (2020). Occurrence and risk assessment of
481 pyrrolizidine alkaloids in spices and culinary herbs from various geographical origins. *Toxins*, *12*, 155.
482 https://doi.org/10.3390/toxins12030155

483 Kapp, T. (2017). *Pyrrolizidine Alkaloids in Culinary Herbs—Take Caution with Borage-Containing*
484 *Herbal Mixes*. Retrieved from https://www.ua-
485 bw.de/pub/beitrag.asp?subid=1&Thema_ID=2&ID=2485&lang=EN&Pdf=No Accessed July 29, 2021.

486 Kapp, T., Hägele, F., & Plate, E.M. (2019). *Oregano—An Aromatic but Loaded Culinary Herb; Part I:*
487 *Pyrrolizidine Alkaloids. CVUA Stuttgart*. Retrieved from
488 https://www.cvuas.de/pesticides/beitrag_en.asp?subid=1&Thema_ID=5&ID=3024&lang=EN&Pdf=N
489 o Accessed July 29, 2021.

490 Lawal, A., Wong, R. C. S., Tan, G. H., Abdulra'uf, L. B., & Alsharif, A. M. A. (2018). Recent
491 modifications and validation of QuEChERS-dSPE coupled to LC–MS and GC–MS instruments for
492 determination of pesticide/agrochemical residues in fruits and vegetables. *J. Chromatogr. Sci.*, *56*, 656-
493 669. https://doi.org/10.1093/chromsci/bmy032

494 Li, Y. F., Qiao, L. Q., Li, F. W., Ding, Y., Yang, Z. J., & Wang, M. L. (2014). Determination of multiple
495 pesticides in fruits and vegetables using a modified quick, easy, cheap, effective, rugged and safe method
496 with magnetic nanoparticles and gas chromatography tandem mass spectrometry. *J. Chromatogr. A*,
497 *1361*, 77-87. https://doi.org/10.1016/j.chroma.2014.08.011

498 Mädge, I., Gehling, M., Schöne, C., Winterhalter, P., & These, A. (2020). Pyrrolizidine alkaloid profiling
499 of four Boraginaceae species from Northern Germany and implications for the analytical scope proposed

for monitoring of maximum levels. *Food Addit. Contam. Part A, 37, 1339-1358.* https://doi.org/10.1080/19440049.2020.1757166

Nowak, M., Wittke, C., Lederer, I., Klier, B., Kleinwächter, M., & Selmar, D. (2016). Interspecific transfer of pyrrolizidine alkaloids: An unconsidered source of contaminations of phytopharmaceuticals and plant derived commodities. *Food Chem.*, *213*, 163-168. https://doi.org/10.1016/j.foodchem.2016.06.069

Oellig, C., & Schmid, S. (2019). Polyethyleneimine as weak anionic exchanger adsorbent for clean-up in pesticide residue analysis of fruits and vegetables. *J. Chromatogr. A, 1597*, 9-17. https://doi.org/10.1016/j.chroma.2019.03.020

Omar, M. M. A., Ibrahim, W. A. W., & Elbashir, A. A. (2014). Sol–gel hybrid methyltrimethoxysilane–tetraethoxysilane as a new dispersive solid-phase extraction material for acrylamide determination in food with direct gas chromatography–mass spectrometry analysis. *Food Chem.*, *158*, 302-309. https://doi.org/10.1016/j.foodchem.2014.02.045

Picron, J. F. (2018). *Pyrrolizidine alkaloids in herbs and related foodstuffs (PASHERBS). RTF Tagged EndNote XML RIS*. Retrieved from https://www.sciensano.be/en/biblio/pyrrolizidine-alkaloids-herbs-and-related-foodstuffs-pasherbs Accessed July 29, 2021.

Picron, J. F., Herman, M., Van Hoeck, E., & Goscinny, S. (2018). Analytical strategies for the determination of pyrrolizidine alkaloids in plant based food and examination of the transfer rate during the infusion process. *Food Chem*., *266*, 514-523. https://doi.org/10.1016/j.foodchem.2018.06.055

Porto-Figueira, P., Camacho, I., & Câmara, J. S. (2015). Exploring the potentialities of an improved ultrasound-assisted quick, easy, cheap, effective, rugged, and safe-based extraction technique combined with ultrahigh pressure liquid chromatography fluorescence detection for determination of Zearalenone in cereals, *J. Chromatogr. A, 1408*, 187–196. https://doi.org/10.1016/j.chroma.2015.07.031

Q2(R1) Validation of Analytical Procedures: Text and Methodology. Guidance for Industry - International Council for Harmonisation. (2005). Retrieved from https://www.fda.gov/regulatory-information/search-fda-guidance-documents/q2r1-validation-analytical-procedures-text-and-methodology-guidance-industry Accessed December 10, 2021.

RASFF—Food and Feed Safety Alerts. (2021). Retrieved from https://webgate.ec.europa.eu/rasff-window/screen/search Accessed July 29, 2021.

Selmar, D., Radwan, A., & Nowak, M. (2015). Horizontal natural product transfer: A so far unconsidered source of contamination of plant-derived commodities. *J. Environ. Anal. Toxicol.*, *5*, 1000287. https://doi.org/10.1007/978-3-319-68717-9_12

Selmar, D., Wittke, C., Beck-von Wolffersdorff, I., Klier, B., Lewerenz, L., Kleinwächter, M., & Nowak, M. (2019). Transfer of pyrrolizidine alkaloids between living plants: A disregarded source of contaminations. *Environ. Pol*., *248*, 456-461. https://doi.org/10.1016/j.envpol.2019.02.026

Uclés, A., López, S. H., Hernando, M. D., Rosal, R., Ferrer, C., & Fernández-Alba, A. R. (2015). Application of zirconium dioxide nanoparticle sorbent for the clean-up step in post-harvest pesticide residue analysis. *Talanta*, *144*, 51-61. https://doi.org/10.1016/j.talanta.2015.05.055

Urban, M., & Lesueur, C. (2017). Comparing d-SPE sorbents of the QuEChERS extraction method and EMR-lipid for the determination of polycyclic aromatic hydrocarbons (PAH_4) in food of animal and plant origin. *Food Anal. Methods*, *10*, 2111-2124. https://doi.org/10.1007/s12161-016-0750-9

Zhao, D., Huo, Q., Feng, J., Chmelka, B. F., & Stucky, G. D. (1998). Nonionic triblock and star diblock copolymer and oligomeric surfactant syntheses of highly ordered, hydrothermally stable, mesoporous silica structures. *J. Am. Chem. Soc.*, *120*, 6024-6036. https://doi.org/10.1021/ja974025i

544 Zhao, P., Wang, L., Zhou, L., Zhang, F., Kang, S., & Pan, C. (2012). Multi-walled carbon nanotubes as
545 alternative reversed-dispersive solid phase extraction materials in pesticide multi-residue analysis with
546 QuEChERS method. *J. Chromatogr. A, 1225*, 17-25. https://doi.org/10.1016/j.chroma.2011.12.070

547 Zheng, H. B., Ding, J., Zheng, S. J., Yu, Q. W., Yuan, B. F., & Feng, Y. Q. (2015). Magnetic "one-step"
548 quick, easy, cheap, effective, rugged and safe method for the fast determination of pesticide residues in
549 freshly squeezed juice. *J. Chromatogr. A, 1398*, 1-10. https://doi.org/10.1016/j.chroma.2015.04.021

550

Figure Captions

Fig. 1 Pyrrolizidine alkaloids included in this work and classified into different families based on their structural similarities and botanical origin.

Fig. 2 (a) 2D plot of the matrix effect of the analytes/retention time obtained in rosemary and basil samples using PSA, LP-MS and LP-MS-NH2 as clean-up sorbents. Recovery percentages obtained from the analysis of **(b)** three spiked replicates of a rosemary sample (100 µg/Kg of each analyte) and **(c)** three spiked replicates of a basil sample (100 µg/Kg of each analyte), extracted by the modified µ-QuEChERS procedure proposed before and after its optimization. Error bars represent the standard deviation of sample replicates (n = 3).

Fig. 3 (a) Heat map plot of the individual content of PAs and PANOs and **(b)** total content of PAs/PANOs (µg/Kg) found in the different aromatic herb samples analyzed by the modified µ-QuEChERS method proposed. In the sample identification code, the first letter indicates: *R* for rosemary, *B* for basil, *T* for thyme, and *H* for herbs de Provence; followed by their type of farming: *C* for conventional, *O* for organic and *W* for wild farming, whereas *I* was for samples collected from plants grown "in-house".

Table 1. Retention time and mass spectrum parameters of the targeted analytes using the UHPLC-IT-MS/MS method developed in positive ESI ion mode.

Analyte	**Retention Time (min)**	**Precursor Ion (*m/z*)**	**Fragmentation Amplitude**	**MS^2. Product Ions [a] (*m/z*)**
Intermedine	5.6	299	0.70	**138**, 120
Europine	5.7	329	0.80	**253**, 138
Lycopsamine	5.8	299	0.70	**138**, 120
Europine *N*-oxide	6.2	345	0.80	**327**, 171.5
Intermedine *N*-oxide	6.4	315	0.80	225, **171.5**
Lycopsamine *N*-oxide	6.5	315	0.80	**171.5**, 138
Retrorsine	6.8	351	0.80	**323**, 275
Retrorsine *N*-oxide	7.0	367	0.90	**339**, 245
Seneciphylline	7.2	333	0.80	**305**, 120
Heliotrine	7.2	313.5	0.70	**138**, 120
Seneciphylline *N*-oxide	7.5	350	0.80	**321**, 118
Heliotrine *N*-oxide	7.6	329	1.00	**171**, 136
Senecivernine	7.9	335	0.80	**307**, 120
Senecionine	7.9	335	0.80	**307**, 120
Senecivernine *N*-oxide	8.1	351	0.80	**323**, 219.5
Senecionine *N*-oxide	8.3	352	1.00	220, **118**
Echimidine	8.7	398	0.60	220, **120**
Echimidine *N*-oxide	8.7	413	0.70	**395**, 351
Senkirkin	9.1	365	0.80	**167.5**, 150
Lasiocarpine	9.8	411	0.70	**335**, 219.5
Lasiocarpine *N*-oxide	10.4	428	0.80	**409**, 352

[a] Predominant product ion. Ions in bold were the ones used for quantification. Isolation width (m/z) is 4. Retention time with the optimized gradient elution: 5% B (0–0.5 min), 5–50% B (0.5–7 min), 50% B (7–7.5 min), 50–100% B (7.5–11 min), 100% B (11–12 min), 100–5% B (12–14 min). Water containing 0.2% formic acid and 5 mM ammonium acetate as mobile phase A and methanol containing 10 mM ammonium acetate as mobile phase B. The flow rate was 0.25 mL/min.

Table 2. Validation parameters of the modified µ-QuEChERS method proposed for the determination of the target PAs/PANOs in rosemary samples.

Analytes	Linear Range (µg/Kg)	Matrix-Matched Calibration R^2	Accuracy		Precision		MDL (µg/Kg)	MQL (µg/Kg)
			Recovery (% ± sd)	Mean Recovery (% ± sd)	Repeatability (RSD%)	Reproducibility (RSD%)		
Intermedine	10.0–500.0	y = 10118x - 56959	82 ± 7 [a]	90 ± 8	14 [a]	17 [a]	2.7	9.1
		0.999	98 ± 2 [b]		9 [b]	11 [b]		
			89 ± 3 [c]		5 [c]	11 [c]		
Europine	10.0–500.0	y = 4796x - 51720	101 ± 7 [a]	80 ± 18	13 [a]	16 [a]	1.2	4.0
		0.998	71 ± 2 [b]		5 [b]	16 [b]		
			69 ± 4 [c]		8 [c]	9 [c]		
Lycopsamine	10.0–500.0	y = 5661x - 39739	104 ± 4 [a]	79 ± 21	10 [a]	10 [a]	2.2	7.2
		0.999	67 ± 0 [b]		8 [b]	12 [b]		
			67 ± 2 [c]		8 [c]	12 [c]		
Europine *N*-oxide	10.0–500.0	y = 13771x - 233753	100 ± 2 [a]	97 ± 3	9 [a]	20 [a]	2.7	9.1
		0.999	94 ± 1 [b]		6 [b]	12 [b]		
			96 ± 5 [c]		7 [c]	9 [c]		
Intermedine *N*-oxide	10.0–500.0	y = 9911x - 131545	101 ± 3 [a]	93 ± 11	11 [a]	16 [a]	2.5	8.3
		0.998	98 ± 3 [b]		5 [b]	7 [b]		
			80 ± 2 [c]		5 [c]	8 [c]		
Lycopsamine *N*-oxide	10.0–500.0	y = 5899x - 70610	99 ± 3 [a]	91 ± 12	9 [a]	14 [a]	1.6	5.3
		0.998	96 ± 0 [b]		11 [b]	11 [b]		
			77 ± 1 [c]		14 [c]	16 [c]		
Retrorsine	10.0–500.0	y = 86x + 11503	103 ± 1 [a]	101 ± 7	14 [a]	19 [a]	2.9	9.6
		0.999	107 ± 2 [b]		14 [b]	16 [b]		
			94 ± 4 [c]		7 [c]	19 [c]		
Retrorsine *N*-oxide	10.0–500.0	y = 955x - 11899	101 ± 4 [a]	103 ± 3	8 [a]	9 [a]	2.7	9.2
		0.999	106 ± 1 [b]		18 [b]	19 [b]		
			102 ± 6 [c]		8 [c]	17 [c]		
Seneciphylline	10.0–500.0	y = 2129x - 5999	98 ± 4 [a]	86 ± 12	13 [a]	16 [a]	2.8	9.4
		0.999	87 ± 9 [b]		13 [b]	15 [b]		
			74 ± 0 [c]		11 [c]	17 [c]		
Heliotrine	10.0–500.0	y = 22260x + 82018	93 ± 2 [a]	95 ± 2	17 [a]	17 [a]	0.7	2.5
		0.999	96 ± 0 [b]		16 [b]	16 [b]		
			95 ± 4 [c]		10 [c]	16 [c]		
Seneciphylline *N*-oxide	10.0–500.0	y = 1314x + 17526	103 ± 5 [a]	99 ± 3	6 [a]	15 [a]	1.3	4.3
		0.999	98 ± 2 [b]		3 [b]	16 [b]		
			97 ± 2 [c]		12 [c]	19 [c]		
Heliotrine *N*-oxide	10.0–500.0	y = 135x + 1294	102 ± 4 [a]	93 ± 8	5 [a]	16 [a]	2.1	6.9
		0.999	86 ± 3 [b]		7 [b]	15 [b]		
			91 ± 2 [c]		14 [c]	17 [c]		

Senecivernine	10.0–500.0	y = 2530x - 49696 0.999	101 ± 5 [a] 100 ± 2 [b] 78 ± 2 [c]	93 ± 13	12 [a] 12 [b] 11 [c]	19 [a] 15 [b] 15 [c]	1.2	4.2
Senecionine	10.0–500.0	y = 2813x - 26048 0.999	103 ± 3 [a] 100 ± 4 [b] 84 ± 0 [c]	96 ± 10	19 [a] 12 [b] 10 [c]	20 [a] 18 [b] 15 [c]	2.4	8.2
Senecivernine *N*-oxide	10.0–500.0	y = 1825x + 2034 0.999	93 ± 1 [a] 93 ± 0 [b] 87 ± 1 [c]	91 ± 3	5 [a] 10 [b] 12 [c]	13 [a] 16 [b] 19 [c]	1.7	5.7
Senecionine *N*-oxide	10.0–500.0	y = 4247x - 40862 0.999	102 ± 4 [a] 100 ± 0 [b] 73 ± 3 [c]	92 ± 16	12 [a] 10 [b] 12 [c]	19 [a] 15 [b] 12 [c]	2.5	8.5
Echimidine	10.0–500.0	y = 85x + 2046 0.999	96 ± 5 [a] 92 ± 4 [b] 99 ± 6 [c]	96 ± 4	11 [a] 12 [b] 9 [c]	18 [a] 20 [b] 10 [c]	2.9	9.6
Echimidine *N*-oxide	10.0–500.0	y = 2012x + 903405 0.998	98 ± 1 [a] 102 ± 2 [b] 101 ± 2 [c]	100 ± 2	16 [a] 14 [b] 6 [c]	19 [a] 14 [b] 19 [c]	3.0	9.9
Senkirkin	10.0–500.0	y = 1293x + 519 0.999	96 ± 2 [a] 97 ± 3 [b] 71 ± 2 [c]	88 ± 15	19 [a] 8 [b] 12 [c]	20 [a] 18 [b] 13 [c]	2.6	8.6
Lasiocarpine	10.0–500.0	y = 1396x - 40299 0.999	91 ± 2 [a] 99 ± 2 [b] 99 ± 1 [c]	96 ± 5	18 [a] 15 [b] 9 [c]	19 [a] 16 [b] 11 [c]	1.5	5.0
Lasiocarpine *N*-oxide	10.0–250.0	y = 4399x - 44162 0.999	98 ± 2 [a] 99 ± 0 [b] 80 ± 3 [c]	92 ± 11	11 [a] 5 [b] 11 [c]	19 [a] 8 [b] 14 [c]	2.8	9.3

Recovery: mean recovery obtained from six samples (n = 6) spiked with the analytes at a known concentration level, and subjected to the proposed extraction procedure; Repeatability: six consecutive injections (n = 6) on the same day of a sample spiked with the analytes at a known concentration level; Reproducibility: three replicates of a sample injected in triplicate throughout three different days (n = 9) and spiked with the analytes at a known concentration level; MDL: method detection limit; MQL: method quantification limit; [a] Low spiked level (10 µg/Kg); [b] Medium spiked level (100 µg/Kg); [c] High spiked level (800 µg/Kg).

Table 3. Validation parameters of the modified µ-QuEChERS method proposed for the determination of the target PAs/PANOs in basil samples.

Analytes	Linear Range (µg/Kg)	Matrix-Matched Calibration R^2	Accuracy		Precision		MDL (µg/Kg)	MQL (µg/Kg)
			Recovery (% ± sd)	Mean Recovery (% ± sd)	Repeatability (RSD%)	Reproducibility (RSD%)		
Intermedine	10.0–500.0	y = 10259x - 130642	101 ± 2 [a]	92 ± 11	18 [a]	18 [a]	3.0	9.8
		0.999	80 ± 2 [b]		3 [b]	15 [b]		
			96 ± 5 [c]		8 [c]	18 [c]		
Europine	10.0–500.0	y = 6139x - 12675	99 ± 4 [a]	98 ± 6	14 [a]	15 [a]	2.4	7.9
		0.999	92 ± 7 [b]		11 [b]	17 [b]		
			103 ± 1 [c]		7 [c]	15 [c]		
Lycopsamine	10.0–500.0	y = 6337x - 102712	97 ± 2 [a]	88 ± 10	16 [a]	18 [a]	3.0	10.0
		0.999	78 ± 4 [b]		13 [b]	17 [b]		
			89 ± 1 [c]		6 [c]	14 [c]		
Europine *N*-oxide	10.0–500.0	y = 12199x - 47148	100 ± 5 [a]	93 ± 13	11 [a]	16 [a]	2.9	9.6
		0.999	78 ± 6 [b]		3 [b]	12 [b]		
			101 ± 0 [c]		8 [c]	17 [c]		
Intermedine *N*-oxide	10.0–500.0	y = 12283x - 103692	99 ± 1 [a]	89 ± 9	10 [a]	15 [a]	1.5	5.1
		0.999	85 ± 4 [b]		5 [b]	10 [b]		
			82 ± 7 [c]		8 [c]	9 [c]		
Lycopsamine *N*-oxide	10.0–500.0	y = 7959x - 93111	97 ± 2 [a]	88 ± 8	4 [a]	20 [a]	0.7	2.2
		0.999	86 ± 10 [b]		15 [b]	18 [b]		
			81 ± 1 [c]		7 [c]	14 [c]		
Retrorsine	10.0–500.0	y = 95x + 1349	104 ± 6 [a]	103 ± 2	6 [a]	15 [a]	2.8	9.3
		0.999	103 ± 3 [b]		11 [b]	20 [b]		
			101 ± 1 [c]		7 [c]	15 [c]		
Retrorsine *N*-oxide	10.0–500.0	y = 198x + 3626	99± 6 [a]	100 ± 1	17 [a]	19 [a]	2.8	9.5
		0.999	100 ± 5 [b]		18 [b]	19 [b]		
			100 ± 5 [c]		15 [c]	18 [c]		
Seneciphylline	10.0–500.0	y = 2647x - 14743	98 ± 1 [a]	97 ± 1	15 [a]	15 [a]	2.5	8.3
		0.999	96 ± 2 [b]		10 [b]	11 [b]		
			97 ± 7 [c]		8 [c]	17 [c]		
Heliotrine	10.0–500.0	y = 31227x - 85693	102 ± 4 [a]	102 ± 4	13 [a]	17 [a]	2.0	6.6
		0.999	105 ± 1 [b]		7 [b]	17 [b]		
			98 ± 4 [c]		13 [c]	19 [c]		
Seneciphylline *N*-oxide	10.0–500.0	y = 2950x - 40067	95 ± 4 [a]	88 ± 9	18 [a]	18 [a]	1.1	3.8
		0.999	91 ± 4 [b]		9 [b]	16 [b]		
			78 ± 6 [c]		13 [c]	19 [c]		
Heliotrine *N*-oxide	10.0–500.0	y = 486x + 11088	96 ± 5 [a]	96 ± 5	19 [a]	20 [a]	2.8	9.2
		0.999	101 ± 3 [b]		14 [b]	17 [b]		
			91 ± 6 [c]		18 [c]	20 [c]		

Senecivernine	10.0–500.0	y = 2094x + 3564 0.999	102 ± 5 [a] 99 ± 3 [b] 96 ± 1 [c]	99 ± 3	13 [a] 11 [b] 6 [c]	15 [a] 19 [b] 11 [c]	2.5	8.3
Senecionine	10.0–500.0	y = 2724x - 24748 0.999	101 ± 4 [a] 99 ± 6 [b] 100 ± 6 [c]	100 ± 1	11 [a] 10 [b] 12 [c]	15 [a] 12 [b] 16 [c]	3.0	10.0
Senecivernine *N*-oxide	10.0–500.0	y = 1626x + 309 0.999	98 ± 4 [a] 95 ± 2 [b] 76 ± 1 [c]	90 ± 12	18 [a] 10 [b] 15 [c]	18 [a] 15 [b] 17 [c]	2.8	9.5
Senecionine *N*-oxide	10.0–500.0	y = 12218x - 218973 0.999	101 ± 3 [a] 98 ± 3 [b] 95 ± 6 [c]	98 ± 3	7 [a] 7 [b] 10 [c]	17 [a] 14 [b] 12 [c]	2.9	9.7
Echimidine	10.0–500.0	y = 126x + 6839 0.999	97 ± 10 [a] 99 ± 2 [b] 101 ± 2 [c]	99 ± 2	9 [a] 16 [b] 14 [c]	18 [a] 17 [b] 20 [c]	1.3	4.3
Echimidine *N*-oxide	10.0–500.0	y = 888x - 5278 0.999	101 ± 3 [a] 103 ± 3 [b] 103 ± 2 [c]	102 ± 1	15 [a] 12 [b] 14 [c]	16 [a] 19 [b] 16 [c]	1.7	5.8
Senkirkin	10.0–500.0	y = 4607x - 9869 0.999	96 ± 1 [a] 98 ± 2 [b] 103 ± 4 [c]	99 ± 4	19 [a] 4 [b] 5 [c]	20 [a] 7 [b] 8 [c]	3.0	10.0
Lasiocarpine	10.0–500.0	y = 1978x - 21551 0.999	104 ± 5 [a] 97 ± 5 [b] 103 ± 3 [c]	101 ± 4	4 [a] 11 [b] 13 [c]	19 [a] 18 [b] 18 [c]	1.2	3.9
Lasiocarpine *N*-oxide	10.0–500.0	y = 37278x - 101868 0.999	100 ± 2 [a] 93 ± 4 [b] 93 ± 4 [c]	95 ± 4	11 [a] 3 [b] 5 [c]	11 [a] 10 [b] 9 [c]	2.8	9.3

Recovery: mean recovery obtained from six samples (n = 6) spiked with the analytes at a known concentration level, and subjected to the proposed extraction procedure; Repeatability: six consecutive injections (n = 6) on the same day of a sample spiked with the analytes at a known concentration level; Reproducibility: three replicates of a sample injected in triplicate throughout three different days (n = 9) and spiked with the analytes at a known concentration level; MDL: method detection limit; MQL: method quantification limit; [a] Low spiked level (10 µg/K); [b] Medium spiked level (100 µg/Kg); [c] High spiked level (800 µg/Kg).

Table 4. Validation parameters of the modified µ-QuEChERS method proposed for the determination of the target PAs/PANOs in thyme samples.

Analytes	Linear Range (µg/Kg)	Matrix-Matched Calibration R^2	Accuracy		Precision		MDL (µg/Kg)	MQL (µg/Kg)
			Recovery (% ± sd)	Mean Recovery (% ± sd)	Repeatability (RSD%)	Reproducibility (RSD%)		
Intermedine	10.0–500.0	y = 7744x - 117703	80 ± 8 [a]	88 ± 8	8 [a]	17 [a]	2.9	9.7
		0.999	95 ± 1 [b]		11 [b]	16 [b]		
			90 ± 3 [c]		9 [c]	10 [c]		
Europine	10.0–500.0	y = 4522x - 55375	99 ± 7 [a]	86 ± 15	7 [a]	18 [a]	2.9	9.5
		0.999	88 ± 2 [b]		6 [b]	20 [b]		
			70 ± 3 [c]		5 [c]	7 [c]		
Lycopsamine	10.0–500.0	y = 5103x - 56892	63 ± 4 [a]	73 ± 8	10 [a]	16 [a]	2.5	8.3
		0.999	77 ± 1 [b]		10 [b]	13 [b]		
			78 ± 1 [c]		3 [c]	9 [c]		
Europine *N*-oxide	10.0–500.0	y = 10367x - 84394	96 ± 1 [a]	84 ± 12	12 [a]	20 [a]	1.4	4.6
		0.999	82 ± 2 [b]		12 [b]	15 [b]		
			73 ± 4 [c]		8 [c]	8 [c]		
Intermedine *N*-oxide	10.0–500.0	y = 10213x - 124188	75 ± 6 [a]	81 ± 7	15 [a]	17 [a]	2.7	9.1
		0.999	79 ± 4 [b]		11 [b]	17 [b]		
			89 ± 7 [c]		5 [c]	7 [c]		
Lycopsamine *N*-oxide	10.0–500.0	y = 6870x - 99410	99 ± 7 [a]	82 ± 19	13 [a]	19 [a]	0.9	3.1
		0.999	75 ± 1 [b]		14 [b]	18 [b]		
			72 ± 0 [c]		5 [c]	9 [c]		
Retrorsine	10.0–500.0	y = 55x - 333	93 ± 7 [a]	97 ± 4	14 [a]	20 [a]	2.7	9.1
		0.998	100 ± 5 [b]		16 [b]	18 [b]		
			98 ± 4 [c]		17 [c]	20 [c]		
Retrorsine *N*-oxide	10.0–500.0	y = 761x + 19568	98 ± 8 [a]	100 ± 4	17 [a]	19 [a]	1.6	5.4
		0.999	97 ± 2 [b]		18 [b]	20 [b]		
			105 ± 6 [c]		7 [c]	7 [c]		
Seneciphylline	10.0–500.0	y = 1540x - 13245	104 ± 10 [a]	95 ± 12	16 [a]	16 [a]	2.3	7.3
		0.999	99 ± 2 [b]		11 [b]	17 [b]		
			81 ± 6 [c]		14 [c]	16 [c]		
Heliotrine	10.0–500.0	y = 26759x - 150017	92 ± 8 [a]	92 ± 8	11 [a]	11 [a]	2.1	7.0
		0.999	100 ± 1 [b]		4 [b]	14 [b]		
			85 ± 4 [c]		9 [c]	10 [c]		
Seneciphylline *N*-oxide	10.0–500.0	y = 1078x - 14069	90 ± 6 [a]	90 ± 10	8 [a]	17 [a]	2.8	9.2
		0.999	99 ± 1 [b]		11 [b]	16 [b]		
			80 ± 9 [c]		9 [c]	10 [c]		
Heliotrine *N*-oxide	10.0–500.0	y = 313x + 5661	95 ± 4 [a]	98 ± 3	8 [a]	11 [a]	0.4	1.2
		0.999	97 ± 5 [b]		17 [b]	18 [b]		
			101 ± 12 [c]		8 [c]	12 [c]		

Senecivernine	10.0–500.0	y = 2612x - 34693 0.999	94 ± 10 [a] 106 ± 6 [b] 68 ± 7 [c]	89 ± 19	18 [a] 10 [b] 9 [c]	19 [a] 18 [b] 13 [c]	2.2	7.4
Senecionine	10.0–500.0	y = 2534x - 21778 0.999	100 ± 3 [a] 102 ± 0 [b] 76 ± 0 [c]	93 ± 14	15 [a] 13 [b] 9 [c]	16 [a] 16 [b] 14 [c]	1.9	6.3
Senecivernine *N*-oxide	10.0–500.0	y = 1098x + 375 0.999	96 ± 3 [a] 96 ± 2 [b] 73 ± 7 [c]	88 ± 13	17 [a] 5 [b] 14 [c]	20 [a] 14 [b] 15 [c]	1.9	6.5
Senecionine *N*-oxide	10.0–500.0	y = 8706x - 103321 0.999	93 ± 5 [a] 96 ± 6 [b] 65 ± 7 [c]	85 ± 17	3 [a] 8 [b] 6 [c]	10 [a] 13 [b] 10 [c]	2.5	8.3
Echimidine	10.0–500.0	y = 456x - 3313 0.999	120 ± 1 [a] 92 ± 2 [b] 102 ± 4 [c]	105 ± 14	3 [a] 8 [b] 17 [c]	3 [a] 10 [b] 17 [c]	2.6	8.8
Echimidine *N*-oxide	10.0–500.0	y = 887x + 26203 0.998	98 ± 5 [a] 100 ± 1 [b] 104 ± 7 [c]	101 ± 3	11 [a] 15 [b] 6 [c]	11 [a] 19 [b] 19 [c]	2.5	8.2
Senkirkin	10.0–500.0	y = 10120x - 79673 0.999	100 ± 5 [a] 99 ± 4 [b] 85 ± 2 [c]	95 ± 8	19 [a] 10 [b] 5 [c]	20 [a] 17 [b] 12 [c]	1.8	6.0
Lasiocarpine	10.0–500.0	y = 267x - 3099 0.999	111 ± 5 [a] 99 ± 2 [b] 98 ± 2 [c]	103 ± 7	15 [a] 13 [b] 15 [c]	19 [a] 18 [b] 18 [c]	2.3	7.6
Lasiocarpine *N*-oxide	10.0–500.0	y = 31643x - 231921 0.999	100 ± 6 [a] 91 ± 1 [b] 75 ± 6 [c]	89 ± 13	8 [a] 4 [b] 2 [c]	9 [a] 12 [b] 8 [c]	2.8	9.2

Recovery: mean recovery obtained from six samples (n = 6) spiked with the analytes at a known concentration level, and subjected to the proposed extraction procedure; Repeatability: six consecutive injections (n = 6) on the same day of a sample spiked with the analytes at a known concentration level; Reproducibility: three replicates of a sample injected in triplicate throughout three different days (n = 9) and spiked with the analytes at a known concentration level; MDL: method detection limit; MQL: method quantification limit; [a] Low spiked level (10 µg/Kg); [b] Medium spiked level (100 µg/Kg); [c] High spiked level (800 µg/Kg).

Fig. 1

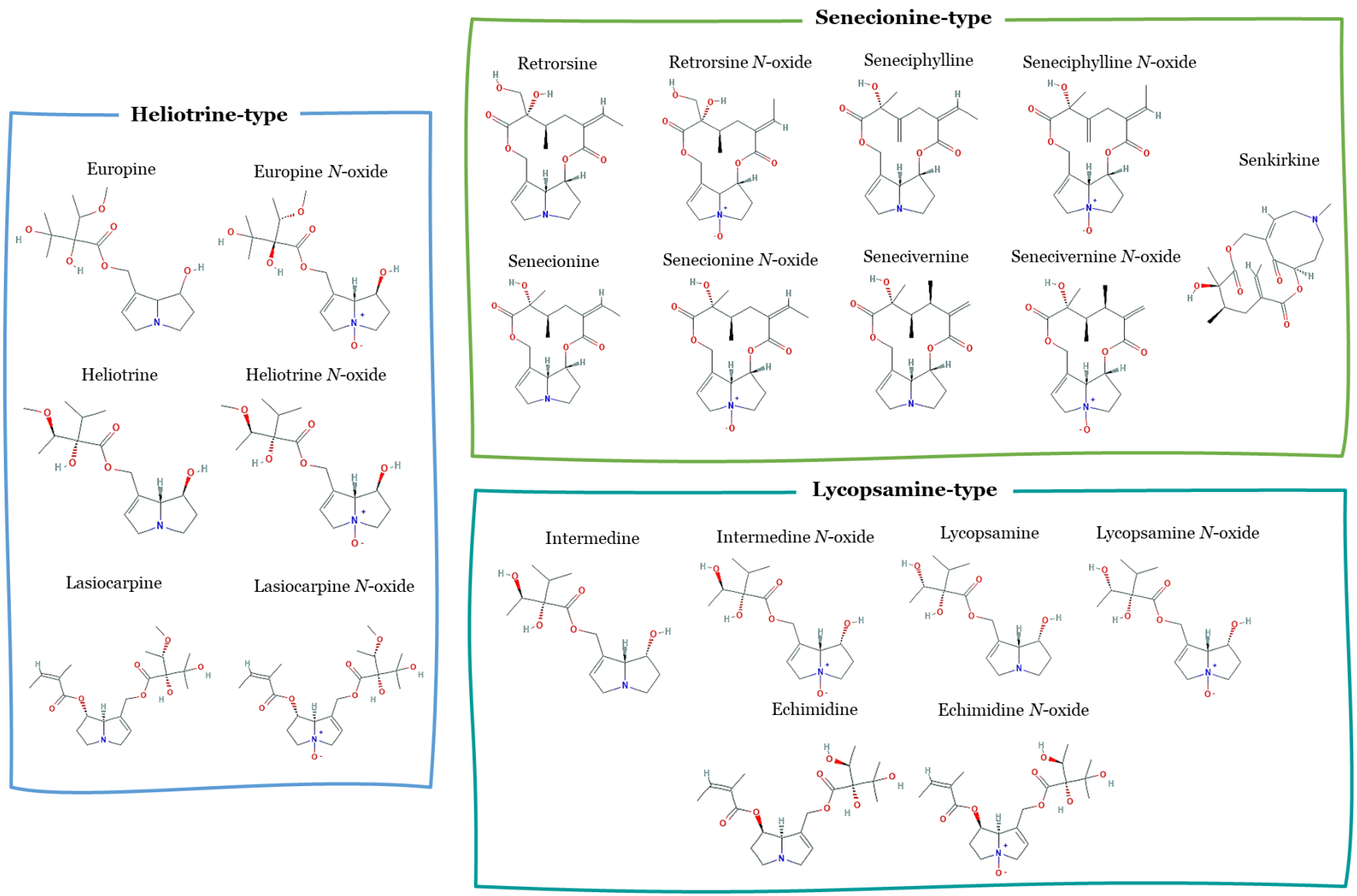
Heliotrine-type
Europine
Europine N-oxide
Heliotrine
Heliotrine N-oxide
Lasiocarpine
Lasiocarpine N-oxide
Senecionine-type
Retrorsine
Retrorsine N-oxide
Seneciphylline
Seneciphylline N-oxide
Senkirkine
Senecionine
Senecionine N-oxide
Senecivernine
Senecivernine N-oxide
Lycopsamine-type
Intermedine
Intermedine N-oxide
Lycopsamine
Lycopsamine N-oxide
Echimidine
Echimidine N-oxide

Fig. 2

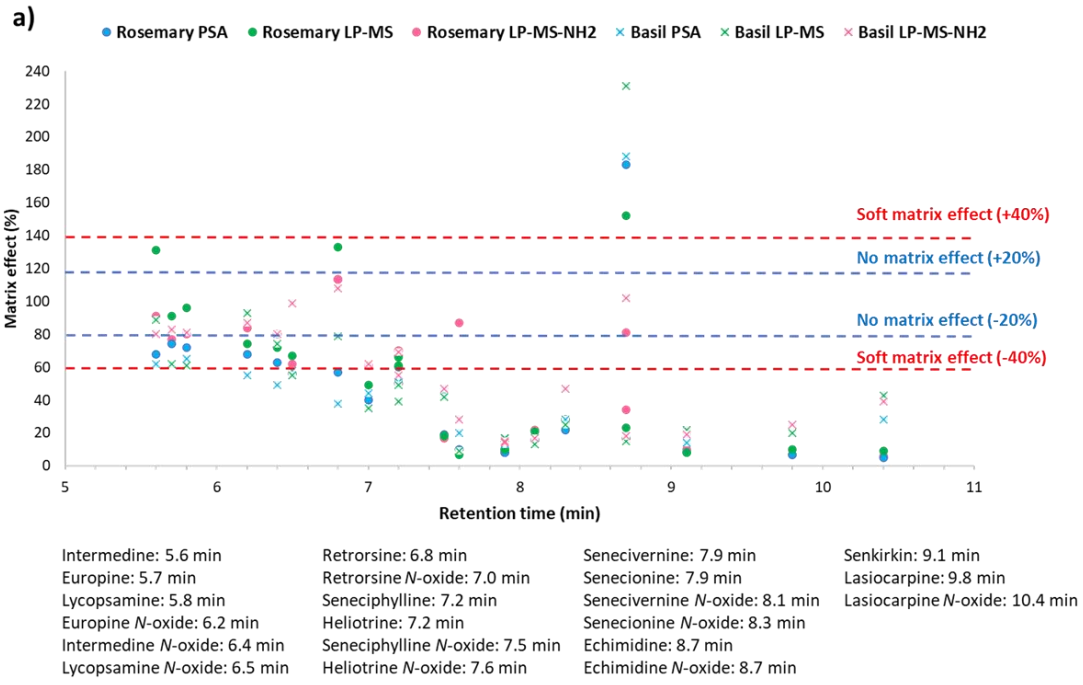
a)
Rosemary PSA
Rosemary LP-MS
Rosemary LP-MS-NH2
Basil PSA
Basil LP-MS
Basil LP-MS-NH2
Matrix effect (%)
Retention time (min)
Soft matrix effect (+40%)
No matrix effect (+20%)
No matrix effect (-20%)
Soft matrix effect (-40%)
Intermedine: 5.6 min
Europine: 5.7 min
Lycopsamine: 5.8 min
Europine N-oxide: 6.2 min
Intermedine N-oxide: 6.4 min
Lycopsamine N-oxide: 6.5 min
Retrorsine: 6.8 min
Retrorsine N-oxide: 7.0 min
Seneciphylline: 7.2 min
Heliotrine: 7.2 min
Seneciphylline N-oxide: 7.5 min
Heliotrine N-oxide: 7.6 min
Senecivernine: 7.9 min
Senecionine: 7.9 min
Senecivernine N-oxide: 8.1 min
Senecionine N-oxide: 8.3 min
Echimidine: 8.7 min
Echimidine N-oxide: 8.7 min
Senkirkin: 9.1 min
Lasiocarpine: 9.8 min
Lasiocarpine N-oxide: 10.4 min

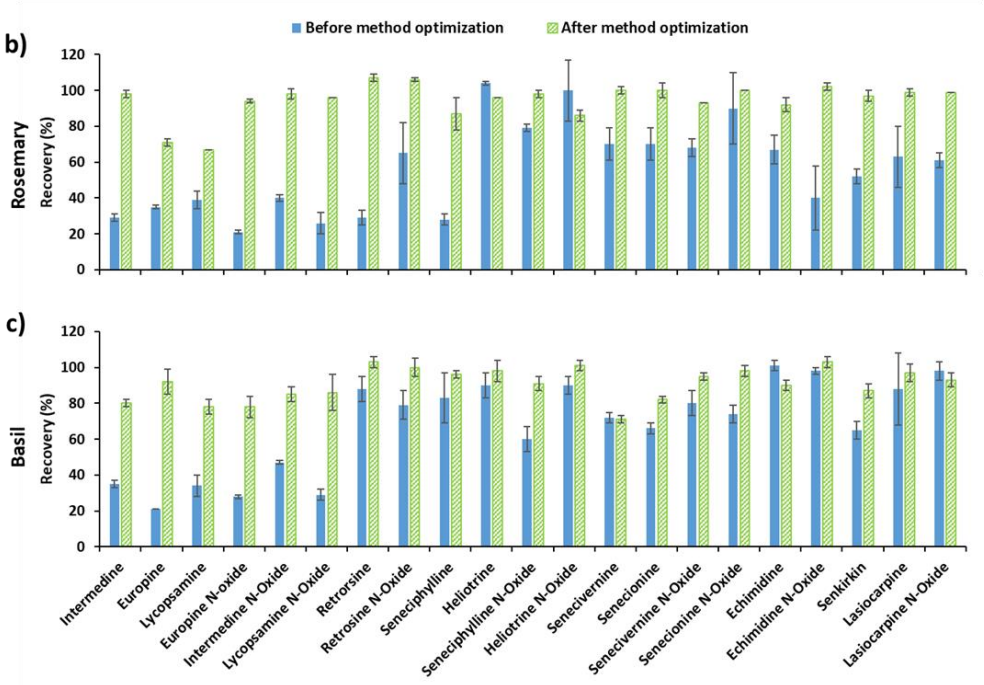
b)
Before method optimization
After method optimization
Rosemary
Recovery (%)
c)
Basil
Recovery (%)
Intermedine
Europine
Lycopsamine
Europine N-oxide
Intermedine N-Oxide
Lycopsamine N-Oxide
Retrorsine
Retrosine N-Oxide
Seneciphylline
Heliotrine
Seneciphylline N-Oxide
Heliotrine N-Oxide
Senecivernine
Senecionine
Senecivernine N-Oxide
Senecionine N-Oxide
Echimidine
Echimidine N-Oxide
Senkirkin
Lasiocarpine
Lasiocarpine N-Oxide

Fig. 3

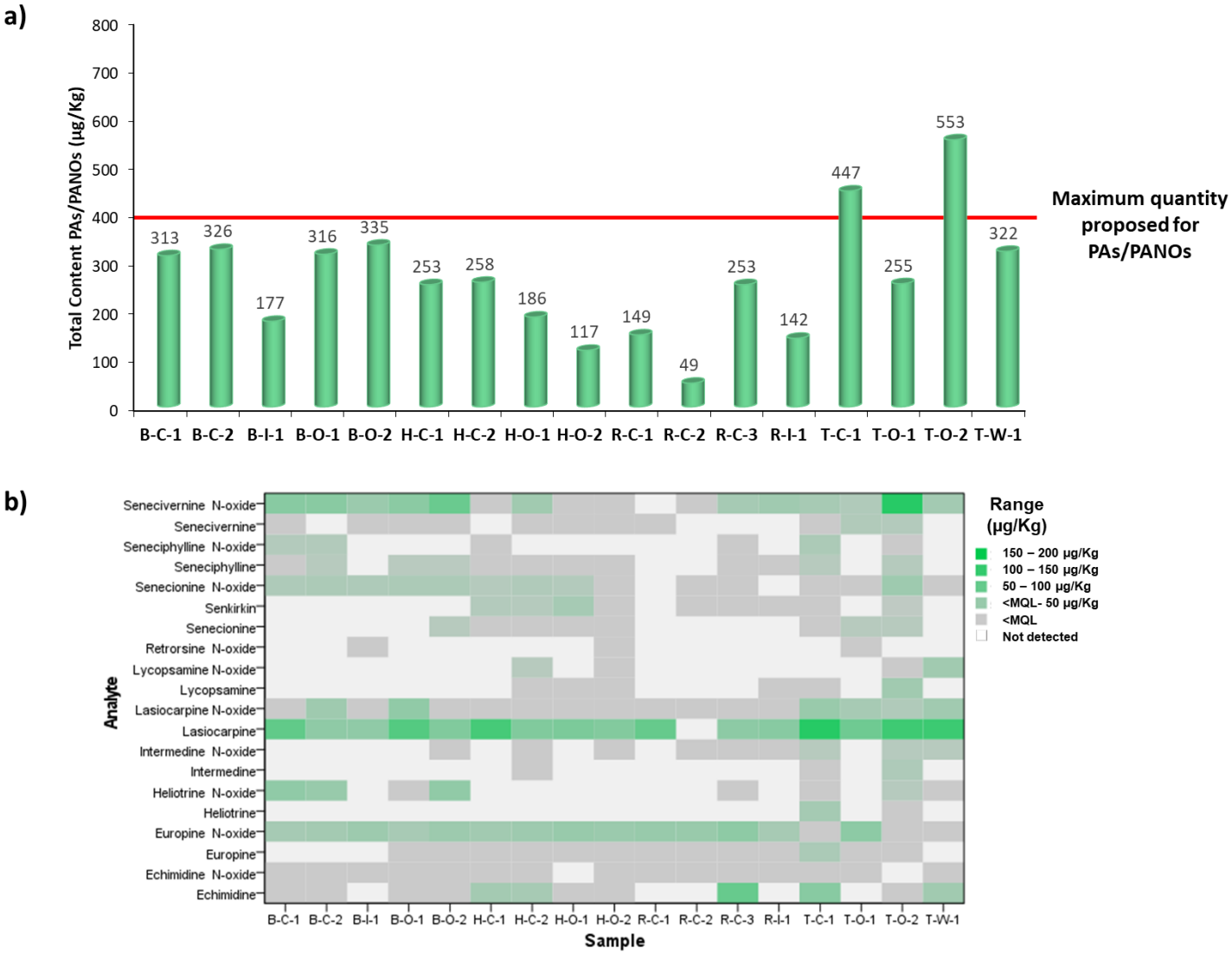
a)
Total Content PAs/PANOs (µg/Kg)
800
700
600
500
400
300
200
100
0
313
326
177
316
335
253
258
186
117
149
49
253
142
447
255
553
322
Maximum quantity proposed for PAs/PANOs
B-C-1 B-C-2 B-I-1 B-O-1 B-O-2 H-C-1 H-C-2 H-O-1 H-O-2 R-C-1 R-C-2 R-C-3 R-I-1 T-C-1 T-O-1 T-O-2 T-W-1
b)
Senecivernine N-oxide
Senecivernine
Seneciphylline N-oxide
Seneciphylline
Senecionine N-oxide
Senkirkin
Senecionine
Retrorsine N-oxide
Lycopsamine N-oxide
Lycopsamine
Lasiocarpine N-oxide
Lasiocarpine
Intermedine N-oxide
Intermedine
Heliotrine N-oxide
Heliotrine
Europine N-oxide
Europine
Echimidine N-oxide
Echimidine
Analyte
B-C-1 B-C-2 B-I-1 B-O-1 B-O-2 H-C-1 H-C-2 H-O-1 H-O-2 R-C-1 R-C-2 R-C-3 R-I-1 T-C-1 T-O-1 T-O-2 T-W-1
Sample
Range (µg/Kg)
150 – 200 µg/Kg
100 – 150 µg/Kg
50 – 100 µg/Kg
<MQL- 50 µg/Kg
<MQL
Not detected

Supplementary material

Miniaturized and modified QuEChERS method with mesostructured silica as clean-up sorbent for pyrrolizidine alkaloids determination in aromatic herbs

Sergio Izcara, Natalia Casado, Sonia Morante-Zarcero, Damián Pérez-Quintanilla, Isabel Sierra*

Departamento de Tecnología Química y Ambiental, E.S.C.E.T, Universidad Rey Juan Carlos, C/ Tulipán s/n, 28933 Móstoles, Madrid, Spain

* Corresponding author: Tel.: (+34) 914887018; fax: (+34) 914888143.

E-mail addresses: sergio.izcara@urjc.es; natalia.casado@urjc.es; sonia.morante@urjces; damian.perez@urjc.es; isabel.sierra@urjc.es

SM1. Characterization of LP-SM and LP-SM-NH_2 mesostructured silicas

The materials were characterized in terms of transmission electron microscopy (TEM), scanning electron microscopy (SEM) and nitrogen gas adsorption-desorption isotherms. The TEM measures were done using, a JEOL F200 ColdFEG microscope operating at 200 kV with a resolution of 0.23 nm with a microanalysis module EDS JEOL with Centurio detector of 100 mm^2 and a digital camera One View of GATAN. The samples were dispersed in acetone and placed in a Cu grip with a layer of perforated C. For SEM, a Nova Nano SEM 230 FEI microscope was used. Previously, the samples were prepared with a sputtering method using a sputter coater BAL-TEC SCD 005 as follows: sputter time 100 s, sputter current 30 mA and film thickness 7 nm of gold. Nitrogen gas adsorption-desorption isotherms were carried out on a Micromeritics ASAP 2020 analyzer. Additionally, elemental analysis (% N) was performed on LP-SM-NH_2 to estimate the functionalization degree of amino groups attached to the silica, using a microanalyser model Flash 2000 Thermo Fisher Scientific Inc.

The TEM micrographs of the synthesized materials displayed a perfect pore size distribution in a three-dimensional network, wormhole type. The open-pore network has a homogenous pore size distribution being accessible through the whole particle of the mesostructured silica. SEM micrographs revealed low dispersion particle size with quasi-spherical, spherical, or amorphous shape, with an average size of 100 nm. The particles tend to form clusters or agglomerates with sizes between 1-3 µm common in some silica-based materials. According to the I.U.P.A.C classification, the nitrogen gas adsorption-desorption isotherms of both silicas were of type IV showing an H1 hysteresis loop, which is usual in materials with cylindrical pores of constant cross-section. The isotherms showed several steps: the first step until relative pressure (P/P_0) 0.5 that indicates monolayer adsorption, then at relative pressures between 0.5 and 0.7 takes places the

multi-layer adsorption, between 0.7 and 0.95 the capillary condensation inside the pores of the material and, finally, at higher relative pressures the adsorption on the surface of the material.

Textural properties of both materials are typical of surfactant-assembled mesostructures and verify the uniform framework mesoporosity of the materials synthesized. It was successfully confirmed the large pore volume of the silicas, as the pore volume values obtained (1.74 - 1.18 cm^3/g) are higher than the ones for conventional mesostructured silicas. Likewise, the pore size distribution of the materials (calculated with the Barrett-Joyner-Halenda (BJH) method using the desorption branch of the isotherm) was also higher, showing a bimodal pore distribution with the main pore centered at 150 Å , and the second one at 90 Å (in the case of LP-MS). After the modification process, both pore diameters decreased, being higher in the bigger one, as a consequence of a higher functionalization due to its better accessibility and efficient mass-transfer process of the ligand inside-outside the pore in the modification step. The attachment of the amino groups was verified with the % N obtained through elemental analysis, which enabled to estimate the functionalization degree of LP-MS-NH_2

Textural properties of the materials synthesized

Mesostructured silica	S_{BET} [a] (m^2/g)	Pore Volume (cm^3/g)	BJH [b] pore diameter (Å)	L_0 (mmol amino groups/g material)[c]
LP-MS	522	1.74	150/90	-
LP-MS-NH_2	340	1.18	124/89	1.04

[a] S_{BET}: Specific surface area calculated by Brunauer-Emmett-Teller (BET) method
[b] BJH: Pore size distribution calculated using Barrett-Joyner-Halenda (BJH) method in the desorption branch
[c] Functionalization degree of amino groups = (%N × 10)/14

Table S1. Information of the aromatic herb samples analyzed.

Sample	Product origin	Raw material origin	Description
R-C-1	Spain	Unknown	Milled rosemary leaf (*Rosmarinus officinalis*)
R-C-2	Spain	Unknown	Milled rosemary leaf (*Rosmarinus officinalis*)
R-C-3	Spain	Unknown	Milled rosemary leaf (*Rosmarinus officinalis*)
R-I-1	Spain	Spain	Rosemary grown "in-house" (*Rosmarinus officinalis*)
B-C-1	Spain	Unknown	Milled basil leaf (*Ocimum basilicum*)
B-C-2	Spain	Egypt	Milled basil leaf (*Ocimum basilicum*)
B-O-1	France	Unknown	Milled basil leaf from organic farming (*Ocimum basilicum*)
B-O-2	Spain	Unknown	Milled basil leaf from organic farming (*Ocimum basilicum*)
B-I-1	Spain	Spain	Basil grown "in-house" (*Ocimum basilicum*)
T-C-1	Spain	Spain	Milled thyme leaf (*Thymus vulgaris*)
T-O-1	France	Unknown	Milled thyme leaf from organic farming (*Thymus vulgaris*)
T-O-2	Spain	Unknown	Milled thyme leaf from organic farming (*Thymus vulgaris*)
T-W-1	Spain	Spain	Wild thyme on branch (*Thymus vulgaris*)
H-C-1	Spain	Unknown	Milled herbs de Provence (*Satureja hortensis, Rosmarinus officinalis, Ocimum basilicum, Origanum vulgare*)
H-C-2	France	Unknown	Milled herbs de Provence (*Satureja hortensis, Rosmarinus officinalis, Ocimum basilicum, Origanum vulgare, Origanum majorana*)
H-O-1	France	Unknown	Milled herbs de Provence (*Satureja hortensis, Rosmarinus officinalis, Ocimum basilicum, Origanum vulgare, Thymus vulgaris*) from organic farming
H-O-2	Spain	Unknown	Milled herbs de Provence (*Satureja hortensis, Rosmarinus officinalis, Origanum vulgare, Thymus vulgaris, Hyssopus officinalis, Origanum majorana*) from organic farming

Table S2. Analytical parameters of the modified µ-QuEChERS method proposed for the determination of the target PAs/PANOs in herbs de Provence samples

Analytes	**Linear Range (µg/kg)**	**Matrix-Matched Calibration, R^2**	**Recovery (% ± sd)**	**MDL (µg/kg)**	**MQL (µg/kg)**
Intermedine	10.0–500.0	*y* = 9446*x* - 94096 0.999	89 ± 2	2.9	9.8
Europine	10.0–500.0	y = 4700x - 34849 0.999	88 ± 3	2.4	7.8
Lycopsamine	10.0–500.0	y = 6258x - 105617 0.999	99 ± 1	2.0	6.8
Europine *N*-oxide	10.0–500.0	y = 12129x - 131592 0.999	96 ± 1	2.7	8.9
Intermedine *N*-oxide	10.0–500.0	y = 10315x - 109295 0.999	98 ± 3	2.8	9.2
Lycopsamine *N*-oxide	10.0–500.0	y = 7669x - 113615 0.999	99 ± 3	2.4	8.1
Retrorsine	10.0–500.0	y = 94x + 1966 0.999	96 ± 7	2.5	8.2
Retrorsine *N*-oxide	10.0–500.0	y = 1106x - 44992 0.999	98 ± 3	3.0	10.0
Seneciphylline	10.0–500.0	y = 2529x - 42762 0.999	97 ± 1	1.9	6.4
Heliotrine	10.0–500.0	y = 30318x - 43353 0.999	82 ± 1	2.5	8.5
Seneciphylline *N*-oxide	10.0–500.0	y = 2447x + 77738 0.999	100 ± 4	2.9	9.6
Heliotrine *N*-oxide	10.0–500.0	y = 338x + 2678 0.999	96± 1	1.9	6.5
Senecivernine	10.0–500.0	y = 2391x - 27615 0.999	79 ± 5	2.7	9.1
Senecionine	10.0–500.0	y = 2188x - 24085 0.999	80 ± 5	2.0	6.5
Senecivernine *N*-oxide	10.0–500.0	y = 1586x + 4472 0.999	97 ± 4	2.5	8.2
Senecionine *N*-oxide	10.0–500.0	y = 8466x - 134524 0.999	95 ± 1	2.1	7.0
Echimidine	10.0–500.0	y = 153x - 1202 0.999	103 ± 2	2.2	7.3

Echimidine *N*-oxide	10.0–500.0	y = 2673x + 208480 0.999	101 ± 3	1.8	5.9
Senkirkin	10.0–500.0	y = 2323x - 28876 0.999	100 ± 1	2.4	7.9
Lasiocarpine	10.0–500.0	y = 869x + 78 0.999	90± 5	2.8	9.2
Lasiocarpine *N*-oxide	10.0–250.0	y = 7008x - 80060 0.999	94 ± 4	2.8	9.2

Recovery: mean recovery obtained from six samples (n = 6) spiked with the analytes at a known concentration level (100 µg/kg), and subjected to the proposed extraction procedure; MDL: method detection limit; MQL: method quantification limit.

Table S3. Solvent-based calibrations (R^2) and matrix effects (ME) calculated for the target compounds in rosemary and basil samples.

Analyte	**Solvent-based calibration (R^2)**	**Rosemary**			**Basil**		
		ME [a] (%)	**ME [b] (%)**	**ME [c] (%)**	**ME [a] (%)**	**ME [b] (%)**	**ME [c] (%)**
Intermedine	y = 20502x + 91927 (0.999)	68	131	91	62	89	80
Europine	y = 43117x + 42511 (0.999)	74	91	77	62	62	83
Lycopsamine	y = 15490x + 54630 (0.999)	72	96	80	65	61	81
Europine *N*-oxide	y = 69157x + 50258 (0.999)	68	74	84	55	93	87
Intermedine *N*-oxide	y = 24117x +20670 (0.999)	63	72	80	49	74	80
Lycopsamine *N*-oxide	y = 18251x + 142531 (0.999)	56	67	62	58	55	99
Retrorsine	y = 719x + 17758 (0.999)	57	133	113	38	79	108
Retrorsine *N*-oxide	y = 4519x + 24279 (0.999)	40	49	61	44	35	62
Seneciphylline	y = 25500x + 154863 (0.999)	50	61	70	51	39	55
Heliotrine	y = 49653x + 316712 (0.999)	60	66	67	54	49	69
Seneciphylline *N*-oxide	y = 15171x + 66411 (0.999)	19	18	17	45	42	47
Heliotrine *N*-oxide	y = 9074x – 47681 (0.999)	10	7	87	20	9	28
Senecivernine	y = 75086x – 186884 (0.999)	8	10	9	13	17	14
Senecionine	y = 75221x – 219174 (0.999)	8	10	8	14	17	15
Senecivernine *N*-oxide	y = 20016x + 171210 (0.999)	16	21	22	17	13	17
Senecionine *N*-oxide	y = 17730x + 176096 (0.999)	22	28	28	28	25	47
Echimidine	y = 1609x + 10823 (0.999)	17	23	34	18	15	18
Echimidine *N*-oxide	y = 490x + 3204 (0.999)	183	152	81	188	231	102
Senkirkin	y = 35592x – 49230 (0.999)	8	8	10	14	22	19
Lasiocarpine	y = 9257x + 111871 (0.999)	7	10	7	25	20	25
Lasiocarpine *N*-oxide	y = 170286x -317715 (0.999)	5	9	6	28	43	39

[a] ME: matrix effects expressed as the ratio between the slopes of matrix-matched calibration curves (using PSA as clean-up sorbent) and solvent-based calibration curves.

[b] ME: matrix effects expressed as the ratio between the slopes of matrix-matched calibration curves (using LP-MS as clean-up sorbent) and solvent-based calibration curves.

[c] ME: matrix effects expressed as the ratio between the slopes of matrix-matched calibration curves (using LP-MS-NH_2 as clean-up sorbent) and solvent-based calibration curves.

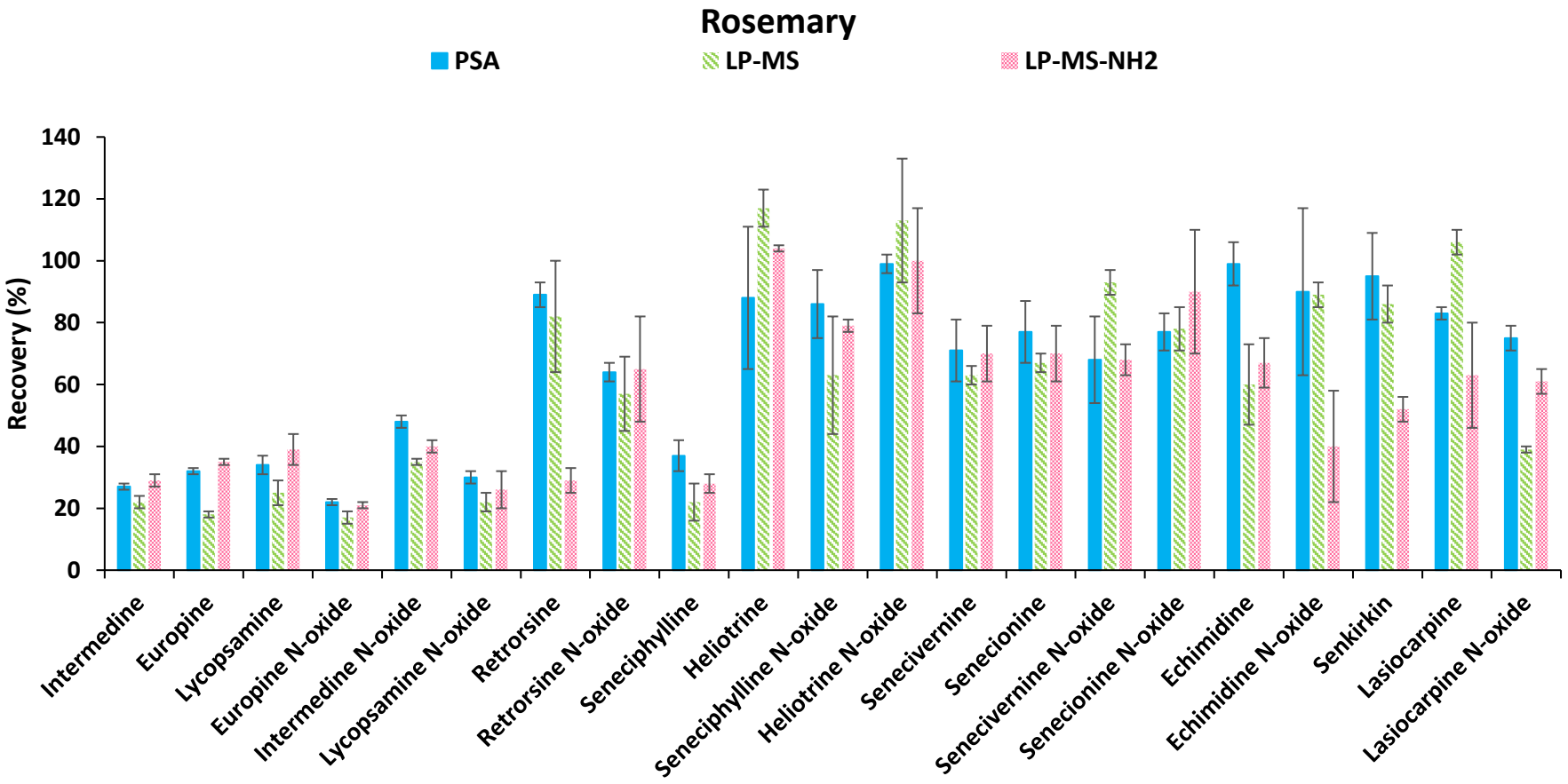

Fig. S1 Comparison of the recovery percentages obtained from the analysis of a spiked rosemary sample (100 µg/kg of each analyte) extracted with the modified µ-QuEChERS procedure proposed before its optimization using PSA, LP-MS and LP-MS-NH_2 as clean-up sorbents. Error bars represent the standard deviation of samples replicates (n = 3).

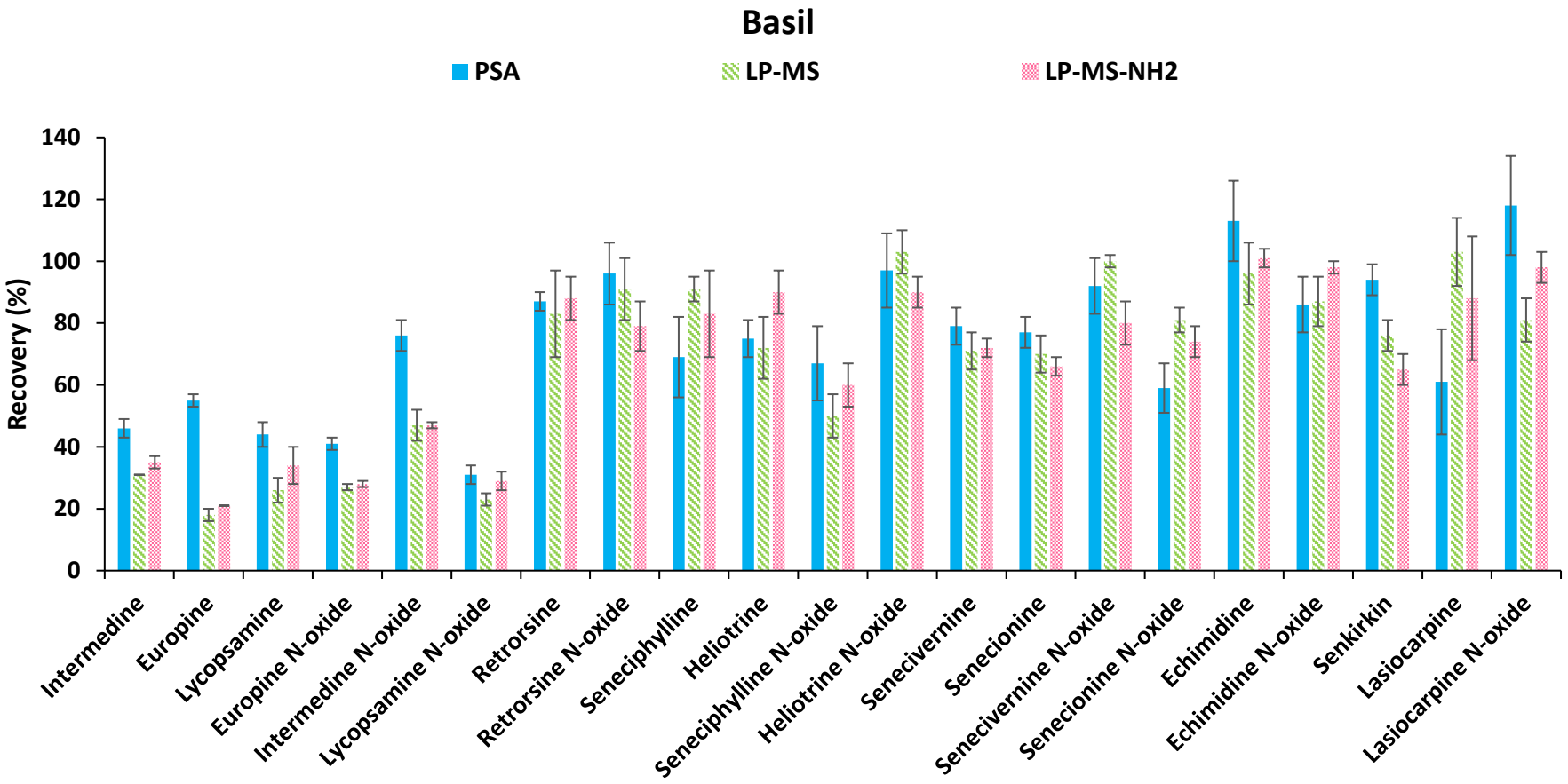

Fig. S2 Comparison of the recovery percentages obtained from the analysis of a spiked basil sample (100 µg/kg of each analyte) extracted with the modified µ-QuEChERS procedure proposed before its optimization using PSA, LP-MS and LP-MS-NH_2 as clean-up sorbents. Error bars represent the standard deviation of samples replicates (n = 3).

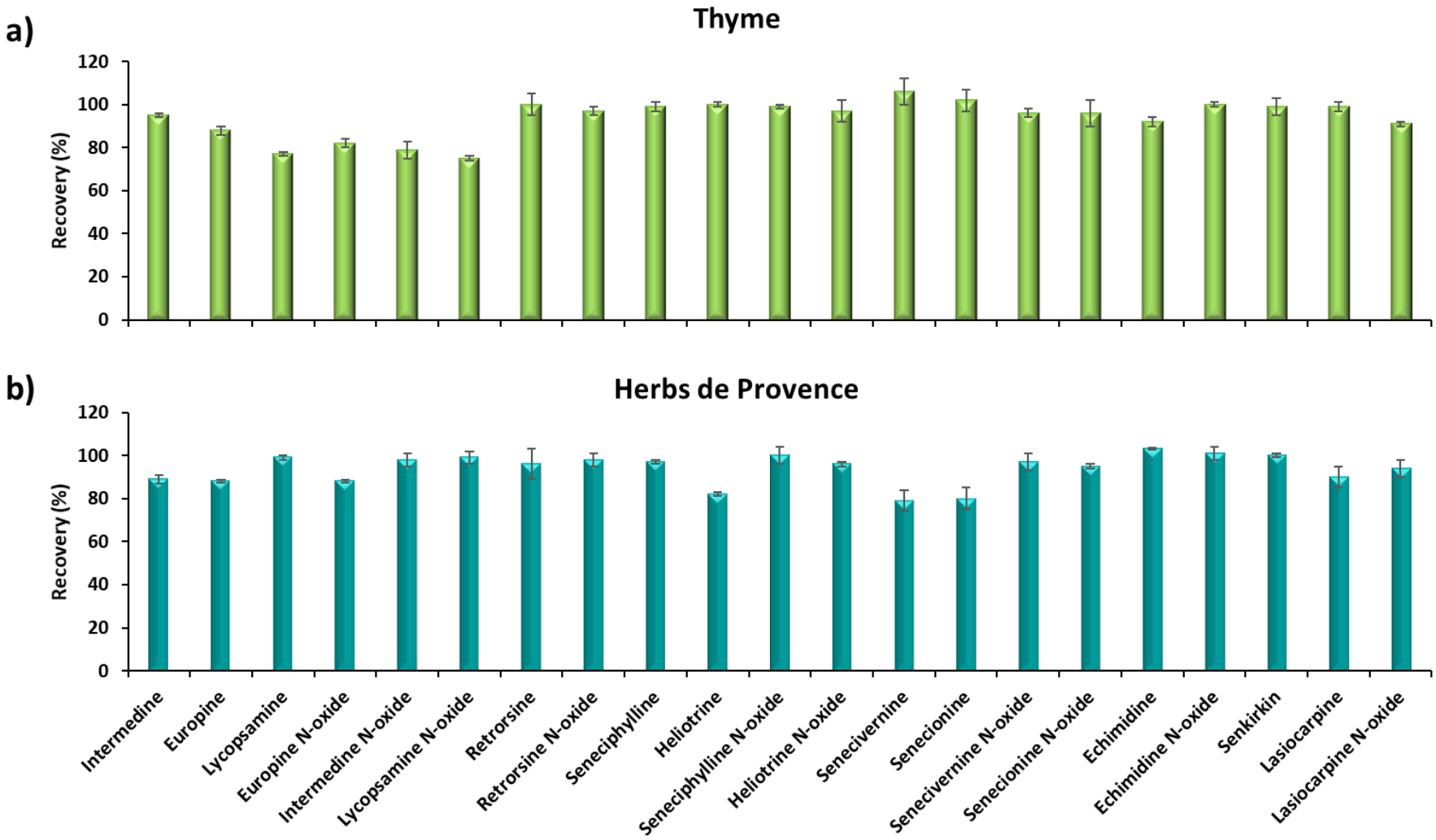

Fig. S3 Recovery percentages obtained from the analysis of **(a)** three spiked replicates of a thyme sample (100 µg/kg of each analyte) and **(b)** three spiked replicates of an herb de Provence sample (100 µg/kg of each analyte), extracted by the final modified µ-QuEChERS procedure proposed. Error bars represent the standard deviation of sample replicates (n = 3).

Table S4. Content of the target PAs/PANOs (µg/Kg) quantified in the different aromatic herbs samples analyzed by the modified µ-QuEChERS method proposed.

Analytes	**R-C-1**	**R-C-2**	**R-C-3**	**R-I-1**	**B-C-1**	**B-C-2**	**B-O-1**	**B-O-2**	**B-I-1**
Intermedine	n.d.	n.d.	n.d.	n.d.	n.d.	n.d.	n.d.	n.d.	n.d.
Europine	<MQL	<MQL	<MQL	<MQL	n.d.	n.d.	<MQL	<MQL	n.d.
Lycopsamine	n.d.	n.d.	n.d.	<MQL	n.d.	n.d.	n.d.	n.d.	n.d.
Europine N-oxide	$50 \pm 1^{a}_{d}$	$49 \pm 3^{a}_{d}$	$59 \pm 3^{b}_{e}$	$35 \pm 2^{a}_{a}$	$36 \pm 4^{b}_{a}$	$38 \pm 3^{c}_{a,b}$	$34 \pm 6^{b}_{a}$	$47 \pm 5^{c}_{d}$	$45 \pm 2^{b}_{c,d}$
Intermedine N-oxide	n.d.	<MQL	<MQL	<MQL	n.d.	n.d.	n.d.	<MQL	n.d.
Lycopsamine N-oxide	n.d.	n.d.	n.d.	n.d.	n.d.	n.d.	n.d.	n.d.	n.d.
Retrorsine	n.d.	n.d.	n.d.	n.d.	n.d.	n.d.	n.d.	n.d.	n.d.
Retrorsine N-oxide	n.d.	n.d.	n.d.	n.d.	n.d.	n.d.	n.d.	n.d.	<LOQ
Seneciphylline	n.d.	n.d.	<MQL	<MQL	<MQL	$19 \pm 2^{a}_{a,b}$	$17 \pm 5^{a}_{a,b}$	$16 \pm 2^{a}_{a}$	n.d.
Heliotrine	n.d.	n.d.	n.d.	n.d.	n.d.	n.d.	n.d.	n.d.	n.d.
Seneciphylline N-oxide	n.d.	n.d.	<MQL	n.d.	$23 \pm 1^{a}_{a}$	$24 \pm 2^{a,b}_{a}$	n.d.	n.d.	n.d.
Heliotrine N-oxide	n.d.	n.d.	<MQL	n.d.	$57 \pm 11^{c}_{b}$	$50 \pm 17^{d}_{b}$	<MQL	$56 \pm 20^{c}_{b}$	n.d.
Senecivernine	<MQL	<MQL	n.d.	n.d.	<MQL	n.d.	<MQL	<MQL	<MQL
Senecionine	n.d.	n.d.	n.d.	n.d.	n.d.	n.d.	n.d.	$19 \pm 3^{a}_{a}$	n.d.
Senecivernine N-oxide	n.d.	<MQL	$36 \pm 13^{a}_{a,b}$	$42 \pm 10^{b}_{a,b}$	$65 \pm 6^{d}_{d}$	$64 \pm 5^{e}_{d}$	$62 \pm 4^{c}_{c,d}$	$95 \pm 17^{e}_{e}$	$47 \pm 10^{b}_{b,c}$
Senecionine N-oxide	n.d.	<MQL	<MQL	n.d.	$28 \pm 3^{a}_{b}$	$30 \pm 1^{b}_{b}$	$30 \pm 1^{b}_{b}$	$30 \pm 2^{b}_{b}$	$28 \pm 2^{a}_{b}$
Echimidine	n.d.	n.d.	$98 \pm 3^{c}_{c}$	n.d.	<MQL	<MQL	<MQL	<MQL	n.d.
Echimidine N-oxide	<MQL	<MQL	<MQL	<MQL	<MQL	<MQL	<MQL	<MQL	<MQL
Senkirkin	n.d.	<MQL	<MQL	<MQL	n.d.	n.d.	n.d.	n.d.	n.d.
Lasiocarpine	$99 \pm 7^{b}_{c,d,e}$	n.d.	$60 \pm 15^{b}_{a}$	$65 \pm 7^{c}_{a}$	$104 \pm 13^{e}_{d,e}$	$58 \pm 2^{e}_{a}$	$117 \pm 24^{d}_{e,f}$	$72 \pm 1^{d}_{a,b}$	$57 \pm 7^{c}_{a}$
Lasiocarpine N-oxide	<MQL	<MQL	<MQL	<MQL	<MQL	$43 \pm 3^{c}_{c}$	$56 \pm 7^{c}_{e}$	<MQL	<MQL
Total	149 ± 35	49 ± 3	253 ± 26	142 ± 16	313 ± 30	326 ± 16	316 ± 36	335 ± 29	177 ± 12

Table S4. (Continued)

Analytes	T-C-1	T-O-1	T-O-2	T-W-1	H-C-1	H-C-2	H-O-1	H-O-2
Intermedine	<LOQ	n.d.	$28 \pm 6^{c}_{a}$	n.d.	n.d.	<LOQ	n.d.	n.d.
Europine	$31 \pm 1^{b}_{a}$	<LOQ	<LOQ	n.d.	<LOQ	<LOQ	<LOQ	<LOQ
Lycopsamine	<LOQ	n.d.	$41 \pm 9^{d}_{a}$	n.d.	n.d.	<LOQ	<LOQ	<LOQ
Europine N-oxide	<LOQ	$60 \pm 9^{d}_{e}$	<LOQ	<LOQ	$40 \pm 4^{b}_{a,b,c}$	$44 \pm 1^{c}_{b,c,d}$	$50 \pm 4^{c}_{d}$	$47 \pm 1^{a}_{d}$
Intermedine N-oxide	$19 \pm 3^{a}_{a}$	n.d.	$20 \pm 3^{b,c}_{a}$	$18.9 \pm 0.3^{a}_{a}$	n.d.	<LOQ	n.d.	<LOQ
Lycopsamine N-oxide	n.d.	n.d.	<LOQ	$41 \pm 2^{b}_{b}$	n.d.	$19 \pm 2^{a}_{a}$	n.d.	<LOQ
Retrorsine	n.d.	n.d.	n.d.	n.d.	n.d.	n.d.	n.d.	n.d.
Retrorsine N-oxide	n.d.	<LOQ	n.d.	n.d.	n.d.	n.d.	n.d.	<LOQ
Seneciphylline	$19 \pm 7^{a}_{a,b}$	n.d.	$21 \pm 3^{b,c}_{b}$	n.d.	<LOQ	<LOQ	<LOQ	<LOQ
Heliotrine	$37 \pm 5^{b}_{a}$	n.d.	<LOQ	n.d.	n.d.	n.d.	n.d.	n.d.
Seneciphylline N-oxide	$30 \pm 5^{b}_{b}$	n.d.	<LOQ	n.d.	<LOQ	n.d.	n.d.	n.d.
Heliotrine N-oxide	<LOQ	n.d.	$20 \pm 6^{b,c}_{a}$	<LOQ	n.d.	n.d.	n.d.	n.d.
Senecivernine	<LOQ	$25 \pm 3^{b}_{a}$	$23 \pm 4^{b,c}_{a}$	n.d.	n.d.	<LOQ	<LOQ	<LOQ
Senecionine	<LOQ	$19 \pm 3^{a}_{a}$	$19 \pm 5^{b,c}_{a}$	n.d.	<LOQ	<LOQ	<LOQ	<LOQ
Senecivernine N-oxide	$35 \pm 9^{b}_{a,b}$	$26 \pm 3^{b}_{a}$	$161 \pm 24^{f}_{f}$	$39 \pm 3^{b}_{a,b}$	<LOQ	$41 \pm 7^{c}_{a,b}$	<LOQ	<LOQ
Senecionine N-oxide	<LOQ	<LOQ	$44 \pm 7^{d}_{c}$	<LOQ	$21 \pm 1^{a}_{a}$	$26 \pm 1^{a}_{b}$	$22.9 \pm 0.2^{a}_{a}$	<LOQ
Echimidine	$65 \pm 10^{d}_{b}$	n.d.	<LOQ	$41 \pm 13^{b}_{a}$	$38 \pm 2^{b}_{a}$	$35 \pm 5^{b,c}_{a}$	<LOQ	<LOQ
Echimidine N-oxide	<LOQ	<LOQ	n.d.	<LOQ	<LOQ	<LOQ	n.d.	<LOQ
Senkirkin	<LOQ	n.d.	$11 \pm 3^{a,b}_{a}$	n.d.	$23 \pm 3^{a}_{b}$	$21 \pm 1^{a}_{b}$	$36 \pm 6^{b}_{c}$	<LOQ
Lasiocarpine	$162 \pm 13^{e}_{h}$	$90 \pm 10^{e}_{b,c,d}$	$139 \pm 12^{e}_{f,g}$	$141 \pm 9^{c}_{g,h}$	$131 \pm 16^{c}_{f,g}$	$72 \pm 25^{d}_{a,b}$	$77 \pm 16^{d}_{a,b,c}$	$70 \pm 9^{b}_{a,b}$
Lasiocarpine N-oxide	$49 \pm 3^{c}_{d}$	$35 \pm 6^{c}_{b}$	$26 \pm 2^{c}_{a}$	$41 \pm 2^{b}_{c}$	<LOQ	<LOQ	<LOQ	<LOQ
Total	447 ± 45	255 ± 27	553 ± 48	350 ± 41	253 ± 46	258 ± 18	186 ± 23	117 ± 16

n.d. = not detected; <MQL: below the limit of quantification of the method. In the sample identification code, the first letter indicates: C for conventional farming, O for organic farming and W for wild farming. Different superscript letters in the same column indicate significant differences ($p < 0.05$) among PAs/PANOs in each sample. Different superscript letters in the same row indicate significant differences ($p < 0.05$) among samples.